Bernal, N. F., Gleeson, S. A., Smith, M. P., Barnes, J. D., Pan, Y. (2017): Evidence of multiple halogen sources in scapolites from iron oxide-copper-gold (IOCG) deposits and regional NaCl metasomatic alteration, Norrbotten County, Sweden. - *Chemical Geology*, *451*, pp. 90—103.

DOI: http://doi.org/10.1016/j.chemgeo.2017.01.005

Evidence of multiple halogen sources in scapolites from iron oxide-copper-gold (IOCG) deposits and regional Na-Cl metasomatic alteration, Norrbotten County, Sweden

Nelson F. Bernal[a*], Sarah A. Gleeson[abc], Martin P. Smith[d], Jaime D. Barnes[e] and Yuanming Pan[f]

[a] University of Alberta, Department of Earth and Atmospheric Sciences.
Edmonton T6G 2E3, Canada.
bernal@ualberta.ca
[b] Helmholtz Centre Potsdam. GFZ German Research Centre for Geosciences, Telegrafenberg B121, Potsdam14473, Germany
sgleeson@gfz-potsdam.de
[c] Institute of Geological Sciences, Freie Universität Berlin, Malteserstrasse 74-100, 12249, Berlin, Germany
[d] School of Environment and Technology, University of Brighton, Cockcroft Building, Lewes Road, Brighton BN2 4GJ, UK
martin.smith@brighton.ac.uk
[e] Department of Geological Sciences, University of Texas, Austin.
Texas 78712, USA
jdbarnes@jsg.utexas.edu
[f] Department of Geological Sciences, University of Saskatchewan, Saskatoon.
Saskatchewan S7N 5E2, Canada
yuanming.pan@usask.ca

*Corresponding author.
Ph: +1(587) 436 1635
Present address:
11 Evansglen Crt NW
Calgary AB, T3P 0P2
Canada.
e-mail:bernal@ualberta.ca

Abstract

Scapolites from barren regional Na-Cl metasomatic assemblages (RM), iron oxide-copper-gold deposits (IOCG), scapolite altered metabasic rocks (IOCG-M), and from IOCG-proximal alteration/Na-skarns (IOCG-PS) from Norrbotten County in Northern Sweden have been analysed for halogen content and Cl stable isotope composition. The aim of the study was to constrain the source of halogens within alteration assemblages, and to investigate the possible fractionation of Cl isotopes between scapolite and the hydrothermal fluid. Scapolite separates were analyzed for Cl, Br, and major oxide concentrations using electron probe micro-analysis (EPMA) and micro-X-ray fluorescence (XRFM) spectrometry. Chlorine was extracted from the scapolite separates via pyrohydrolysis and then analysed for their stable Cl isotope compositions by isotope ratio mass spectrometry (IRMS).

All samples of scapolite investigated in this study are marialitic in composition. One of the scapolites from the Gruvberget deposit (IOCG-PS) had a Cl/Br molar ratio of 2,363, which is the highest amongst all scapolites reported in the literature to date. Cl/Br molar ratios lower than seawater (650), were identified in two IOCG-PS scapolite samples (Cl/Br=554 and 271), as well as in two IOCG-M scapolites (Cl/Br=393 and 565). Three RM scapolites had Cl/Br molar ratios very close to, or slightly higher than, seawater values (639 to 770). Samples with Cl/Br molar ratios less than seawater are inferred to have halogens derived from evaporative residual brines; whereas samples with molar ratios higher than seawater may have halogens derived from fluids that have dissolved halite and/or are from magmatic systems. Considering the wide variation of the Cl/Br molar ratios in the IOCG-PS and IOCG-M scapolites compared to the restricted composition of the regional alteration (RM), it is proposed that the hydrothermal fluids interacted with several different protoliths to generate the IOCG alteration.

RM alteration scapolites had $\delta^{37}Cl$ values from -0.1‰ to +0.3‰, two IOCG-M scapolites had values of 0.2‰ and IOCG-PS scapolites had $\delta^{37}Cl$ values from -0.1‰ to +1.0‰. Using a previously published $\delta^{37}Cl$ value from fluid inclusion leachates (-1.7‰) from the IOCG-M mineralisation at Pahtohavare and the $\delta^{37}Cl$ value of co-existing scapolite measured in this study (0.2‰), an empirical fluid-scapolite fractionation factor was calculated to be +1.9‰. This large fractionation factor is not supported by previous predictions for monovalent chlorides and, assuming equilibrium, indicates that ^{37}Cl was preferentially accommodated in the A site of the scapolite structure. This indicates that either the stable Cl isotope partitioning between the $CaCl_2$-rich brine and the scapolite may differ from currently available estimates for NaCl brines in equilibrium with silicate minerals, or that the scapolite and brine are not in isotopic equilibrium.

Overall, the data in this study suggest that halogens in early scapolites were derived from residual brines and halite, during metamorphism of evaporites linked to the RM alteration. Later in the history of the Norrbotten district components of the RM alteration were recycled and mixed during magmatic and local metasomatic events to varying extents, resulting in the brines associated with IOCG alteration.

Keywords: halogens, chlorine isotopes, isotope fractionation, scapolite, IOCG.

1. Introduction

The ability of the halogen elements to be incorporated in mineral structures is controlled by their ionic radii, electronegativity and electron affinities. In general, F and Cl, with smaller radii and larger electronegativites and electron affinities, are more readily incorporated in non-halide minerals than Br and I. Only a few non-halide minerals can accommodate significant amounts of Cl in their structures, despite the abundance of Cl in some geologic environments. Some of these

Cl-bearing minerals, such as apatite, amphibole, biotite and scapolite, are found in alteration assemblages in ore deposits. Scapolite can also form as a result of metasomatic processes, metamorphism and as a primary phase in igneous rocks (Mora and Valley, 1989; Dong, 2005; Mi and Pan, 2016).

Iron-oxide Cu-Au deposits (IOCG) are found in cratonic areas or on continental margins. These deposits occur in different types of host rocks, including plutonic granitoids, (meta)-andesitic volcanic rocks, and mainly (meta)-siliclastic and/or metabasic rocks (Williams et al., 2005). Fluid inclusion studies on these deposits show that the mineralising fluid is commonly a Cl-rich brine (e.g. Williams et al., 2005; Chiaradia et al. 2006) and the alteration assemblages associated with these deposits often contain Cl-rich scapolite. A variety of fluid sources have been suggested for the brines that form IOCG deposits including magmatic and metamorphic fluids, formation waters and/or mixtures of these end members (e.g. Barton and Johnson, 1996, 2000, Frietsch et al., 1997, Williams et al. 2005, Chiarada et al., 2006, Pollard 2000, 2006, Oliver et al., 2004, Fisher and Kendrick, 2008; Kendrick et al., 2008a).

A temporal and spatial association between the Kiruna type iron oxide-apatite (IOA) and IOCG deposits has been noted in the past (Williams et al. 2005). IOCG deposits are characterized by the occurrence of Cu-sulphide ± Au hydrothermal ores with abundant (> 20%) hematite or magnetite (e.g., Corriveau, 2007; Smith et al., 2012). These deposits are associated with batholitic granitoids and pervasive alkali metasomatism (Williams et al. 2005). A- to I-type magmatism and alkaline-carbonatite stocks may also be related to IOCG mineralisation (Corriveau, 2007). In the Norrbotten region, IOA deposits are restricted to the Kiruna and Galliväre areas, whereas the IOCG deposits are found in the Karelian greenstones and in volcanic rocks of Svecofennian age (Wanhainen at al., 2012).

Gleeson and Smith (2009) determined the halogen contents and Cl stable isotope compositions of fluid inclusions in quartz veins from IOA and IOCG systems in Norrbotten, Sweden. The fluid inclusion leachates from veins in the IOCG deposits had low $\delta^{37}Cl$ values (-5.6‰ to -1.3‰) and it was suggested that the Cl in these fluids had a magmatic, and ultimately a mantle, source but their isotopic composition had been modified by crystallization of scapolites (and micas), which had progressively lowered the $\delta^{37}Cl$ values of the residual fluids. There are no experimental constraints on the direction or magnitude of chlorine isotope fractionation factors between brines and silicate minerals. However, theoretical calculations of equilibrium fractionation of Cl isotopes between solid monovalent chloride NaCl- and KCl-saturated brines and the divalent-metal chlorides $FeCl_2$ and $MnCl_2$, (which may serve as a proxy for the fractionation behavior of structurally bound Cl^- in micas and amphiboles) indicate that ^{37}Cl is partitioned into the divalent chloride (Schauble et al. 2003). The magnitude of the calculated fractionation ranges from 2 to 3‰ at 25 °C to <1‰ at hydrothermal temperatures of 300 to 350 °C. These calculations suggest that there should only be a small partitioning of the ^{37}Cl isotope into amphiboles or micas relative to monovalent chloride brines (e.g. NaCl, KCl). The Cl isotope fractionation between brines and scapolite is unknown, but given that Cl in scapolite is mostly bonded to the monovalent cation Na^+, the theoretical expectation is that scapolite would have less of an affinity for ^{37}Cl than amphiboles or micas. This is due to the control of the Cl oxidation state and its bond partners on calculated fractionation factors (Schauble et al., 2003).

Kusebauch et al. (2015) reported $\delta^{37}Cl$ values of -0.7 to 0.0‰ and or Cl/Br molar ratios of 250 to 143 for scapolites from the Bamble sector, SE Norway. This study discounted the presence of meta-evaporites or mantle sources in the halogen compositions of the fluids in the Bamble sector based on halogen ratios; and instead concluded that the halogens in the scapolites of the Bamble

sector have a marine pore fluid origin. Based on a Rayleigh distillation model, a fractionation factor fluid-scapolite of 1.0010 at 600 °C was identified to explain negative $\delta^{37}Cl$ values measured in the scapolite alteration sequence.

In this study, we have analysed the halogen concentration and the Cl isotope composition of scapolites from the Nunasvaara and, the Greenstone and porphyry-hosted Cu deposits at Pahtohavare, Kallosalmi, Sarkivaara and Gruvberget (Fig. 1). This work tests the hypothesis of Gleeson and Smith (2009), which proposed mantle-derived halogens in the scapolites, and also provides an empirical estimate of the direction and magnitude of the Cl isotope fractionation factor between scapolite and hydrothermal fluids at temperatures between 300-500°C. On the basis of the halogen content and Cl isotope data, the sources of chlorine in scapolite associated with regional metasomatism and ore-forming processes are discussed.

2. Geology background and previous studies

The IOCG-type deposits of Norrbotten County, Sweden (Fig. 1) are hosted by a Paleoproterozoic sequence (~1.9 Ga) of Svecokarelian metavolcanic and metasedimentary rocks known as the Greenstone and Porphyry Groups (Carlon 2000; Bergman et al., 2001). The Karelian Greenstone group is composed of volcanic rocks of tholeiitic to komatiitic composition overlying the Archaean basement (Ekdahl, 1993). The Porphyry Group consists of basalt, trachyandesite and rhyodacite-rhyolite units that are intruded by the syenitic- to quartz syenitic-composition Kiruna porphyries. The Porphyry Group may have acquired their bulk composition as a result of metasomatic overprinting of an older calc-alkaline association (Martinsson, 1997). These units were originally assigned an age of ~1880 Ma (Romer et al., 1994), but U-Pb analyses of cores of titanite grains from the hanging wall to the Luossavaara ore body suggest a minimum age of 2050 Ma (Storey et al., 2007). Albitisation and scapolitisation occurred at a regional scale, but

the timing of regional Na alteration is relatively poorly constrained. Smith et al. (2009) presented a single LA-ICPMS U-Pb age of titanite from Na-altered diorite at Nunasvaara of 1903±8 Ma – an age which is pre- to syn- the main iron-oxide apatite (IOA) mineralisation at Kirunavaara and potentially elsewhere.

IOCG deposits are associated with high salinity brines, which are responsible for the presence of Na-rich alteration, albite and scapolite (Williams et al., 2005; Kendrick et al., 2007; 2008a, b; Gleeson and Smith 2009). The chlorine stable isotope composition and halogen concentrations from fluid inclusion leachates extracted from quartz veins in the region have previously been analysed (Gleeson and Smith, 2009). In the Norrbotten district, some mineralising fluids are Ca-rich. This enrichment is probably due to the dissolution of limestones during the interaction of mineralising fluids with calc-silicate skarns in the area (Wanhainen et al. 2003, Smith et al., 2012). The IOCG alteration, at some locations in the Norrbotten region, is also associated with CO_2-rich hydrothermal fluids and characteristic elemental concentrations that are well understood (Smith et al. 2012).

2.1 Origin of the Samples

Scapolite is directly associated with IOCG mineralisation and also with barren regional units. Scapolite-bearing samples for this study were taken from regional Na-Cl metasomatic assemblages (RM), from scapolite altered metabasic rocks in the vicinity of iron oxide-apatite or iron oxide-copper-gold deposits (IOCG-M), and from intense Na-alteration zones in which the original character of the rock has been obscured by alteration (Na-metasomatites or proximal ‘Na-Skarns’; IOCG-PS) (Fig. 2).

2.1.1 Regional Na-Cl metasomatism (RM)

Regional Na-Cl metasomatism is developed throughout the Norrbotten area, southern Norway and Fennoscandinavia. In the stratigraphy, RM occurs as massive layers and structurally controlled disseminations, stringers and veinlets (Freitsch et al., 1997). Sodium metasomatism in the region has previously been interpreted to be a result of the metamorphism of evaporites in the volcano-sedimentary sequence (Frietsch et al., 1997). In other IOA-IOCG districts, a strong case has been made for the direct association of regional Na-alteration with the mobilisation of metals that are subsequently concentrated in mineral deposits (Barton and Johnson, 1996, 2000; Oliver et al., 2004). The regional metasomatic samples in this study are not associated with ore. Samples were taken from regional alteration assemblages at Nunasvaara, where the contact of a diorite intrusion with brecciated metasediments is exposed. Both the diorite and the host sediments are altered and contain scapolite and albite, with igneous and breccia matrices now dominated by actinolite and abundant accessory titanite (Fig. 2). A second group of samples were taken from well preserved pillow basalts on the banks of the Torneälven River. Here basalts are altered to scapolite-albite-actinolite-bearing assemblages, cut by veins containing scapolite, actinolite, chlorite and magnetite (Fig. 2).

2.1.2 IOCG-Scapolite altered Metabasic Rocks (IOCG-M)

More intense scapolite alteration is developed around many of the ore deposits in the region, typically, but not exclusively, in metabasic protoliths (e.g. Frietsch et al., 1997; Martinsson, 2004; Edfelt et al., 2005; Smith et al., 2007). Samples of scapolite from metabasic hosts in the immediate vicinity of ore deposits were taken from Pahtohavare (Martinsson, 1997; Lindblom et al., 1996) and Kallosalmi (Wägman and Ohlsson, 2000). Pahtohavare is a previously mined Cu-(Au) deposit hosted in folded, greenschist-facies slates and metabasic rocks (Fig. 2). Ore is associated with albitisation and scapolitisation in both lithologies, commonly with overprinting

potassic alteration. Samples were taken from altered metabasic rocks in core, and from a metadolerite dyke exposed in the open pit. Kallosalmi is an unmined prospect in which strongly Na-altered metabasic rocks host carbonate-associated Cu mineralisation. Drill core samples were taken from altered metabasic rocks.

2.1.3 IOCG scapolite rich alteration/Na skarn (IOCG-PS)

Samples were collected from Pahtohavare and Kallosalmi (described above) where intensely scapolitised and albitised rocks with little relict texture directly host chalcopyrite mineralisation (Fig. 3). Similar mineralisation was sampled at Sarkivaara (Wägman and Ohlsson, 2000) where intense scapolite-albite alteration hosts chalcopyrite-molybdenite mineralisation. Samples from Gruvberget (Martinsson and Virkkunen, 2004) were taken from altered metavolcanic rock within 2 m of the contact with a magnetite-hematite-apatite body, with overprinting Cu mineralisation. The alteration consists of the development of albite and scapolite with actinolite, overprinted by K-feldspar alteration (Fig. 2). The rock is also associated with abundant, large (>1cm) titanite crystals. Scapolite and quartz rarely occur directly together, as scapolite occurs as an alteration phase in the wall rock, and the quartz in veins. However, the scapolite alteration in the vicinity of ore deposits is directly associated with chalcopyrite mineralisation, as is quartz at Pahtohavare, Kallosalmi and Gruvberget. Some quartz veins cut scapolite alteration but scapolite, actinolite and quartz have also been observed to co-exist in the same assemblage. The formation of scapolite and quartz is therefore, interpreted to be related to the fluids responsible for mineralization in these deposits.

3. Methods and analytical techniques

Analyses were carried out on scapolite in thin sections and mineral separates. In other to assess the possibility of variable scapolite compositions in the bulk mineral separates, different grain size separates from single samples (100-125μm, 125-250μm, 250-500μm) were analysed for 17 samples (Table 1).

3.1 Electron probe micro-analysis (EPMA)

Electron microprobe analyses of scapolite in thin sections were carried out using a Cameca SX50 electron microprobe at the Natural History Museum, London. Beam conditions were set at 20Kv and 20nA with a spot size of 1mm. Individual elements were calibrated against natural and synthetic mineral standards, including halite for Cl, BaF_2 for F, celestine for S, jadeite for Na, KBr for K, wollastonite for Ca and Si, olivine for Mg, corundum for Al, and pure metal for Fe. Count times were typically 10 s, but were 20 s for the halogens and Na. Background count times were half those on the element peak. The halogens and alkalis were always analysed first to avoid problems of mobility under the electron beam. The data were empirically corrected for peak overlaps using analyses of standards following the techniques outlined in Williams (1996).

3.2 X-ray Fluorescence Microprobe

Bromine analyses were carried out on an XRF Microprobe (XRFM) at the University of Saskatchewan, using the same instrument and analytical protocols described in Pan and Dong (2003). Briefly, the XRF microprobe consists of a 2.0 kW X-ray generator, a concave (Johansson) LiF (220) (R=250 mm) monochromator, a sampler holder attached to a petrographic microscope, and an energy-dispersion X-ray spectrometer. The X-ray generator is operated at a voltage of 45 kV and a current of 20 mA. The X-ray beam (0.1 x 0.5 mm) is focused from the LiF monochromator, and is collimated by a conical collimator of 0.2 x 0.5 mm in dimension. A

calibration curve for Br was first established from four international reference materials: LKSD–1: 11 ppm Br, LKSD–4: 49 ppm Br, NBS1646: 117 ppm Br and MAG–1: 252 ppm Br (Govindaraju, 1994). The calibration curve was further evaluated by using the Br contents in a suite of Cl-rich minerals (i.e., chlorapatite, scapolite and sodalite) determined by instrumental neutron activation analysis (INAA; Pan and Dong, 2003). Scapolite grains of ~100 μm in diameter for X-ray microprobe analyses were carefully selected under a petrographic microscope to minimize mineral and fluid inclusions. The counting times for samples with less than 10 ppm Br, was increased from 10 to 45 minutes. The precision of the method is reflected in the relative standard deviation, which was less than 5% for Br concentrations over 10 ppm, and 10% for concentrations below 10 ppm. The calculated detection limit in the analysis of single mineral grains is ~1 ppm Br (Pan and Dong, 2003).

3.3 Cl extraction by Pyrohydrolysis

Rock samples containing scapolite were crushed and sieved to sizes from 100 to 250 μm. Then single scapolite grains were carefully separated by hand and weighed. Before pyrohydrolysis each sample was cleaned by gently heating the scapolite grains in a HNO_3 solution (Gleeson 2003). After that, the samples were rinsed with deionized water and dried in the oven overnight.

A pyrohydrolysis apparatus was built at the University of Alberta in order to extract the Cl contained in scapolite separates (Fig. 4). The purpose of this technique is to remove the Cl present in the structure of a mineral by melting a small sample mass, we used between 100 and 150 mg of sample separate. The volatiles released during the reaction were carried by a steam flow to a distillation tube obtaining an aqueous solution. The pyrohydrolysis set up used was modified from the one described by Bonifacie et al. (2007) in order to allow for the direct analysis of the Cl concentration in the recovered solution by ion chromatography (IC). The

objective was to avoid the use of a NaOH collecting solution, as further chemical treatment is required to neutralize the high pH of the Cl-bearing solution, potentially leading to contamination. The use of a boiling reservoir and a condensation tube in the present set-up, was modified from the pyrohydrolysis apparatus described in Barnes and Sharp (2006). The boiling reservoir substitutes for a nebulizer, which is used to control the flow of water vapor in other set-ups (i.e. Whitehead and Thomas, 1985; Magenheim et al. 1994; Bonifacie et al. 2007).

The sample was mixed with five parts V_2O_5 (Whitehead and Tomas, 1985), then the mixture was transferred to the reaction tube, which was placed in a position coincident with the central area of the heating element inside the furnace to ensure the homogeneous heating and melting of the sample. Deionized water was heated in the boiling water reservoir, a stream of water steam carried the volatiles from the furnace to the condensation tube where the solution containing Cl^- from the mineral sample is recovered. The total duration of each extraction was 1 hour, including a pre-heating stage from 400 ºC to 1,200 °C of 15 minutes and a melting stage of 45 minutes at 1,200 °C.

Chlorine in scapolites was measured by EPMA in mineral grains and by IC in pyrohydrolysis solutions. Based on the Cl wt % obtained by microprobe analysis, the Cl yield after pyrohydrolysis was calculated (Table 1). Most of the pyrohydrolyzed samples were pure scapolite separates with the exception of sample RM01 (73% scapolite) and three Gruvberget samples (PN14, PN15 and PN16) (34% scapolite) with different grain sizes. The other minerals in these samples are included in Table 1. With the exception of the PN16 sample, the other three samples have a Cl yield of over 100% (112%, 121% and 142%). Errors induced during counting of the scapolite separates could have affected the final yield. Two PN21 samples, had very low yields (24 and 38 %) that were reproduced in several pyrohydrolysis runs. In this case, the source

of error is likely due to a lower percentage of the scapolite grains identified in the sample rather than the efficiency of the Cl extraction method. The efficiency of the pyrohydrolysis extraction was established by using a well characterized biotite sample. This biotite was used as internal standard and was run three times for comparison. The recovered solution was then analysed by IC obtaining Cl yields between 89 and 95% (Table 2). Two types of blanks were analysed to detect any Cl lost. After pyrohydrolysis, the reaction tubes were rinsed with deionized water and then analyzed in the IC. Another blank was taken between runs from the boiling reservoir to assess if any Cl had flowed back from the reaction tube. Chlorine was not detected in any of the blank runs.

3.4 Ion chromatography

Chloride and bromide concentrations in the pyrohydrolysis solutions were analysed at the University of Alberta in the Department of Earth and Atmospheric Sciences using a Dionex DX600 ion chromatograph with an AS-14A analytical column. A seven ion standard, blanks and an internal quality control standard were run along with the samples. Replicate analyses of standards and unknown were also carried out. The reported data have a calculated uncertainty of 5%. The detection limits for Br and Cl were 0.005 ppm.

3.5 Stable Cl isotopes

The Cl extracted from scapolite samples by pyrohydrolysis was contained in an aqueous solution after distillation. The Cl^- in this solution was precipitated as AgCl following the procedures of Eggenkamp (1994) and Magenheim et al. (1994). The solution was reacted with $AgNO_3$ to produce AgCl. The AgCl precipitates were retained on 0.45 µm glass filters and dried overnight. The AgCl samples were then reacted under vacuum with CH_3I at 80 °C for 48 hours to produce

CH_3Cl, the analytical gas. The isotopic compositions were measured on a ThermoElectron MAT 253 mass spectrometer at the University of Texas-Austin under continuous flow. Delta values are reported in standard per mil notation relative to SMOC (standard mean ocean chloride). The precision of the method is ±0.2 ‰ (1σ) based on the long-term reproducibility of three seawater standards and one internal serpentinite standard; the inclusion of the latter, demonstrated that the pyrohydrolysis extraction results in no additional uncertainty.

4. Results

4.1 Major- and trace-element geochemistry of scapolites

4.1.1 Regional Na-Cl Metasomatism (RM)

The Na-Cl metasomatism alteration type is represented by two samples from Nunasvaara and three samples from the Torneälven River outcrops. Sodium oxide is high in sample RM01 (11.99 wt.%). Samples RM07 and RM05 have Na_2O concentrations of 9.27 and 9.00 wt.%, respectively (Table 3 and Fig.5A). Overall, the Nunasvaara and Torneälven RM scapolites are characterized by relatively low CaO, intermediate to low K_2O (0.23 to 0.5 wt.%; Table 3, Fig.5A and B) and low to intermediate SO_4 and Cl contents, (Fig. 6A). Sample RM07 has the highest Fe concentrations of all the samples analysed (Fig. 5B), but its SO_4-CO_3-Cl composition is comparable with all the other Torneälven samples (Fig. 6A). Scapolites related to regional alteration have similar Cl and CO_3 compositions to the proximal metabasites (IOCG-M), but have higher SO_4 contents (Fig. 6A). Scapolites from Nunasvaara have the highest Cl contents in the samples analyzed, ~3.50 wt.% by both XRFM and EPMA (Table 4). In the samples from Nunasvaara, Br was not analyzed.

At Torneälven River the scapolites have similar Cl concentrations (between 2.71 and 2.74 wt.% by EPMA, Table 4). In the Torneälven River samples, Br concentrations vary from 76 to 88 ppm. The Torneälven River samples have similar Cl/Br molar ratios and Br concentrations (Fig. 7). RM scapolites have Cl/Br molar ratios that range from 639 to 770 (Fig. 7).

4.1.2 IOCG-Scapolite altered Metabasic Rocks (IOCG-M)

This alteration type is represented by three samples from Pahtohavare. Sodium oxide concentrations in MB02 and MB11 are similar, 9.36 wt.% (Table 3). The IOCG Metabasic scapolites (IOCG-M) have intermediate CaO concentrations (8.53 to 8.83 wt.%) (Fig. 5A). The IOCG-M scapolites also have high K_2O concentrations, but data were only collected on two samples (Fig. 5B). IOCG-M scapolites also have intermediate Cl concentrations (2.80 wt.%). Samples MB02 and MB11 have low SO_3 contents characteristic of the Pahtohavare scapolites 0.03 and 0.06 wt.%, respectively. Scapolites associated with proximal metabasites (IOCG-M) have low CO_3 contents, which appears to be characteristic of this alteration type (Fig. 6A). Chlorine concentrations are between 2.50 and 2.80 wt.% in samples MB03 and MB10, respectively (Table 4). Sample MB02 (PAH88217 125-250 mm) contains some of the lowest Br concentrations (36 ppm) measured in this set of samples. The IOCG-M samples have a wide range in Cl/Br molar ratios (Fig. 7).

4.1.3 IOCG-Proximal Scapolite-rich alteration/Na-Skarn (IOCG-PS)

The samples of this alteration type come from four deposits: three from Kallosalmi, two from Pahtohavare, four from Gruvberget and one from Sarkivaara. Sodium oxide was only measured in six out of the ten samples from IOCG-PS alteration and ranges from 6.23 wt.% (PN19) to 10.45 wt.% (PN17) (Table 3). The sample with the highest Ca relative to Cl and Na is PN19 (Fig

5A), which belongs to the Sarkivaara deposit. IOCG-PS scapolites vary substantially in Cl and Ca contents. As for the Fe-K-S relationship, the IOCG-PS scapolites from Sarkivaara have the the highest SO_3 (1.05 wt.%), low Cl concentrations (1.00 wt.%) and some of the lowest K_2O concentrations (0.55 wt.%) represented by sample PN19 (Fig. 5B). The Gruvberget scapolites have intermediate to high SO_4 concentrations with low CO_3. Pahtohavare and Kallosalmi scapolites are characterized by low SO_4. Within the IOCG-PS scapolites, the Kallosalmi and the Pahtohavare samples have the highest Cl and CO_3 concentrations, respectively (Fig. 6A). Scapolites associated with proximal ore are divided in two compositional groups, one characterized by high Cl contents and the other with higher SO_4 compositions (Fig. 6A).

All IOCG-PS samples have a range of Cl compositions from 1.00 to 3.33 wt.% (Table 3). Chlorine concentrations in Kallosalmi (PN09, PN20 and PN21) and Pahtohavare (PN17 and PN18) samples are the same (3.30 ppm via XRFM; Table 4). Electron microprobe analysis yielded a higher value for sample PN09 (3.61 wt.%), but lower for sample PN21 (3.09 wt.%). Gruvberget and Sarkivaara samples have the lowest Cl concentrations by both XRFM and EPMA. Chlorine in sample PN19 is particularly low, at 1.00 wt.% by XRFM and 1.32 wt.% by EPMA.

The most remarkable characteristic of the of IOCG-PS scapolites is the high halogen contents detected in two samples. Sample PN19 has the lowest Cl/Br molar ratios of the samples analyzed (271), contrasting with sample PN14 that has the highest (2363), which is the highest amongst all scapolites analyzed in this study and published elsewhere (e.g. Pan and Dong, 2003; Hammerli et al. 2013, 2014) (Table 4).

4.2 Stable Cl isotope Compositions

A scapolite from Nunasvaara belonging to the RM alteration group (RM01) yielded a $\delta^{37}Cl$ value of -0.1‰ (Table 4). Torneälven River samples have $\delta^{37}Cl$ values ranging from 0.0 to +0.3‰. Two scapolite samples from IOCG-M alteration at Pahtohavare yielded values of +0.2‰. Ten scapolite samples from IOCG-PS alteration had $\delta^{37}Cl$ values ranging from -0.1‰ to +1.0‰; the lowest values are from PN15 and PN18, and the highest from PN17. Scapolite samples from Kallosalmi tend to be slightly enriched in ^{37}Cl (+0.4‰ to +0.6‰) compared to Gruvberget scapolites (-0.1‰ to +0.3‰). The Sarkivaara sample has the second highest $\delta^{37}Cl$ value of the IOCG-PS alteration scapolites (+0.9‰).

5. Discussion

5.1 Chemical characteristics of scapolites

The chemical composition of the scapolites analysed indicate that they are all variations of marialite with 1.0 to 3.6 wt % Cl, and 4.6 to 13.6 wt % CaO (Table 3). These ranges are comparable with the compositions of marialites from the Tienshan Fe Skarn deposit, China (Pan and Dong, 2003), the Marcona Magnetite deposit, Peru (Chen et al., 2010), and the Manto Verde IOCG, Chile (Benavides et al., 2007).

The differences in major-element chemistry in combination with the halogen contents of these marialites can provide some constraints on their origin. In Fig. 7, the three groups of scapolites (RM, IOCG-M and IOCG-PS) overlap in the middle of the general trend, where three RM samples are located. The IOCG-PS scapolites encompass almost the entire range of chemical compositions found in the other two mineralisation types; however, these samples are characterized by higher mass percentages of Ca and K. Although the IOCG-PS scapolites do have higher Ca contents, Cl and Na still are the dominant anion and cation.

The variation in S content between alteration types (Fig. 6A and 6B) cannot be a result of progressive removal of S from the fluid in a rock buffered system, nor is S content inherited from precursor phases, so it must reflect variations in fluid composition. The intra-sample variation may be a result of rock buffering of fluid chemistry, but this is not reflected in the Cl-content of the scapolites.

The anion contents of the group of samples investigated (Fig. 6A), represent two compositional trends departing from high Cl concentrations: the Cl-SO_4 trend, defined by the Pahtohavare and Sarkivaara scapolites, and the Cl-CO_3 trend represented by samples from Kallosalmi and Pahtohavare. The scapolites from Nunasvaara follow the Cl-SO_4 trend, whereas scapolites from Torneälven are more related to the Cl-CO_3 trend. Overall, the range of compositions of the IOCG related alteration encompasses that of the regional metasomatic scapolites. Based on the age of the regional alteration at Nunasvaara (1903± 8 Ma) (Smith et al., 2009), it is possible that components from the RM scapolites may have been assimilated or recycled during the intrusion of the magmatic systems that are contemporaneous with IOCG mineralisation, dated at 1.88 to 1.85 Ga (Billström and Martinsson, 2000). This possibility will be explored in the next section in light of the halogen contents of these scapolites.

5.2 Origin of halogens in the Norrbotten Scapolites

We have established from EPMA and XRFM data that overall the Cl composition of the scapolite separates has a range (1.0 to 3.6 wt.%) but this range is much smaller between the different grain size fractions of a single sample (see Table 4). Some separates from the same sample have similar Br concentrations, e.g. the Torneälven river samples and some samples at Kallosalmi and Gruvberget (Table 4) but some of the IOCG-M and IOCG-PS have a wider range, (36 to 143 ppm) and (20 to 134 ppm) respectively. This results in Cl/Br molar ratios that

vary within a single sample in some cases. There is no evidence from the petrographic study or the EPMA data for zoning in single crystals, and thus, we suggest that the variation in Cl/Br molar ratios between splits with different grain sizes represents different scapolite generations within the same sample. In order to assess this possibility future studies should consider the use of micro-analysis of Br on scapolite separates, such as secondary ion mass spectrometry (SIMS).

It has been suggested that the regional scapolites of Norrbotten were formed by low- to medium-grade regional metamorphism of evaporite-bearing assemblages (Frietsch et al., 1997). Experiments with scapolite solid solutions at 750ºC and 4 kbar (Orville, 1975) found that the composition albite + halite favors the formation of marialite ($Na_4Al_3Si_9O_{24}Cl$), which suggests that the occurrence of marialite-rich scapolite is correlated with high NaCl activities. As a result, at these pressure and temperature conditions, Ellis (1978) suggested that regional Cl-rich scapolite is formed from the metamorphism of evaporite beds. In addition, this interpretation has been confirmed by more recent studies that have also suggested that the reaction of plagioclase with halite and calcite during regional metamorphism can generate scapolite (Mora and Valley, 1989; Frietsch et al; 1997). However, the redistribution of Na, Cl and other components during regional metamorphism and circulation of hydrothermal fluids associated with magmatic intrusions has also been recognized as an important process in the Norrbotten region (Frietsch et al., 1997 and references therein). Our data indicates that evaporitic and magmatic fluids can be identified in the halogen and isotopic signatures of the Norrbotten scapolites.

Based on the halogen contents of IOCG-PS scapolites (Fig. 7), two end members are observed, one identified in the Sarkivaara scapolite with the lowest Cl/Br molar ratio (271) representing a residual evaporitic brine, and the other represented by the Gruvberget scapolites with the highest Cl/Br molar ratios (942 to 2,363) suggesting the influence of magmatic fluids. The scapolites

from these two deposits are also characterized by relatively high to intermediate SO_4 and high to intermediate CO_3 contents (Fig. 6A). The halogen compositions of IOCG-M scapolites fall between these two end members, but the samples with low Cl/Br molar ratios have the highest Br contents detected (Table 4). IOCG-M scapolites at Pahtohavare are characterized by low SO_4 and high Cl contents, with a range of low to intermediate CO_3 concentrations (Fig. 6A). RM scapolites from the Torneälven River have low Cl/Br molar ratios (639 to 770) bracketing seawater (650). Although Br was not analysed in samples from Nunasvaara their SO_4-Cl-CO_3 compositions are comparable with the Kallosami, Gruvberget and Pahtohavare scapolites.

Pan and Dong (2003), reported a marialite-fluid halogen distribution coefficient (K_D) of 0.97±0.08. A K_D value close to the unity indicates that the Cl/Br molar ratio of the marialite represents the Cl/Br molar ratio of the hydrothermal fluid. Based on this, we identify the salinity sources of the Norrbotten scapolites.

Following Kesler et al., (1995) formation waters with high Cl/Br and Na/Br ratios (greater than seawater) have been interpreted to contain additional Cl derived from halite dissolution in upper crustal environments. High Cl/Br molar ratios are also typical of magmatic fluids (e.g. Sanjuan et al., 1990, Böhlke and Irwin, 1992; Gleeson and Turner, 2007; Kendrick et al., 2012). A compilation of Cl/Br molar ratios of geothermal fluids associated with magmatic sources suggest that values between 600 and 2000 are indicative of fluids of magmatic origin (Böhlke and Irwin, 1992). More recently, lower Cl/Br molar ratios were measured in fluid inclusion leachates from the Bingham Canyon and the Butte porphyry copper deposits (Nahnybida et al., 2009) extending the magmatic Cl/Br molar value range down to 271. Formation waters with high Br contents and low Cl/Br ratios (less than seawater) are considered to have attained their salinity from a seawater which has undergone evaporation, resulting in the precipitation of halite, leaving the

residual brine enriched in Br (Walter et al., 1990; Kesler et al., 1995). Based on the Cl/Br and Na/Br molar ratios, both evaporated seawater and halite dissolution and/or magmatic sources contribute to the Cl concentration of scapolites from the three types of alteration (RM, IOCG-M and IOCG-PS). However, evaporative residual brines are dominant at Sarkivaara and are also present in some Pahtohavare scapolites (Frietsch et al., 1997). This contrasts with the halogen sources of the regional-scale alteration scapolites from the Bamble Sector, SE Norway, where both magmatic sources and remobilization of meta-evaporites were ruled out on the basis of Br/Cl, I/Cl ratios and stable Cl isotopes, suggesting a marine pore fluid origin (Kusebauch et al. 2015).

As mentioned before, the regional Na-alteration has been dated at 1903 ± 8 Ma (Smith et al., 2009), and predates early Cu-mineralisation, dated from 1.88 to 1.85 Ga (Billström and Martinsson, 2000). The RM scapolites, although from one locality, have a restricted range in compositions unlike the IOCG-related scapolites, which have a wide range of chemical compositions. The early and late Cu-mineralisations in Norrbotten are associated with magmatic intrusions and magmatic-hydrothermal events (Gleeson and Smith 2009). The possible interaction with magmatic-hydrothermal fluids derived from mafic to felsic magmas (Bergman et al. 2001; Kathol and Martinsson, 1999; Romer et al., 1992) in combination with water-rock interaction with a high diversity of protoliths may explain the wide range of chemical compositions found in IOCG scapolites (Figs. 5.5A and 5.5B). Magmatic hydrothermal systems can produce a wide range of Cl/Br molar ratios. In the case of the Bingham Canyon porphyry copper deposit, associated with a mantle-like halogen source, Cl/Br molar ratios range from 535 to 952 (Kendrick et al., 2001). These suggest that pulses of hydrothermal fluid exsolved from a single magmatic source can have different Cl/Br molar ratios.

Two scapolite separates of sample PAH88217, MB02 and MB03, were available for the present study with Cl/Br molar ratios of 1738 and 393, respectively (Table 4). Cl stable isotope analysis was not performed on sample MB03 as there was not enough mineral separate. However, sample MB02, the scapolite separate with the lower Cl/Br molar ratio (1738), reflects a Br depleted source. This characteristic was useful for comparison with the fluid inclusion data in Gleeson and Smith (2009) for sample PAH88217, which was reported with a Cl/Br molar ratio of 5000, also depleted in Br. The isotopic compositions of these two Br depleted samples (mineral and fluid) are discussed in the next section.

5.3 Isotopic fractionation between mineralising fluids and scapolites

The distribution of $\delta^{37}Cl$ values vs Cl/Br molar ratios (Fig. 8) shows that some scapolites from all three alteration types plot within the evaporite field. However, the data from most of the scapolite samples analysed in the present study plot outside both the magmatic and evaporative brine fields. Ten of these scapolites have Cl/Br molar ratios higher than seawater (650), potentially derived from halite dissolution or magmatic hydrothermal systems and do not support a pristine magmatic origin for the scapolite-forming fluid (Fig. 8). However, to assess the original $\delta^{37}Cl$ values in the hydrothermal fluid, it is important to have an understanding of the chlorine isotope fractionation between the fluid and the scapolite.

A previous study on fluid inclusion leachates obtained a range of predominantly negative $\delta^{37}Cl$ values for fluid inclusions in the Norrbotten area (Gleeson and Smith, 2009). These values range from -5.6 to -1.3‰ in Greenstone- and Porphyry-hosted Cu-Au deposits and between -2.4 to +0.5‰ for Cu-Au deposits in the Nautanen Deformation Zone (NDZ). Overall, the majority of the samples had $\delta^{37}Cl$ values ranging from -3.5 to 0‰. These authors suggested that the lowest values were produced by fractionation processes between the hydrothermal fluids and minerals,

like scapolite, in the alteration assemblages. This means that the scapolite would be enriched in ^{37}Cl compared to the co-existing fluid. The analysed fluid inclusions were from quartz veins spatially related to scapolite-bearing alteration (Gleeson and Smith, 2009). Scapolite hosted fluid inclusions were not identified in our study. It is unknown if isotopic equilibrium was attained between the two phases; however, the presence of a scapolite-quartz-actinolite assemblage in sample PAH88217 (Fig. 9) suggests these phases were in textural equilibrium. The present study attempts to quantify the Cl isotope fractionation factor between scapolite and fluid as we have analysed scapolite from the alteration selvage of a quartz vein sample with a known fluid inclusion composition (PAH 88217; Table 1).

If equilibrium was attained in the formation of the hydrothermal scapolite, Rayleigh fractionation calculations can model the evolution of fluid $\delta^{37}Cl$ values measured in fluid inclusions from IOCG deposits at Norrbotten (Gleeson and Smith, 2009). More recently, fractionation calculations have been used to model $\delta^{37}Cl$ values measured in scapolite and amphibole alteration minerals associated with a shear zone in the Bamble sector, SE Norway (Kusebauch et al. 2015). In Kusebauch et al. (2015), the initial and remaining $\delta^{37}Cl$ values of the hydrothermal fluid are calculated assuming theoretical fractionation factors and measured $\delta^{37}Cl$ values in bulk-rock, amphibole and scapolite. This work concludes that the observed decrease in $\delta^{37}Cl$ values in the bulk-rock with increasing distance to a shear zone can be explained by a Rayleigh fractionation or a combination of Rayleigh and kinetic fractionation. Unlike this study, in the present work, the $\delta^{37}Cl$ value of both fluid and scapolite are available for one sample (PAH88217), which allows for a discussion on the potential isotopic exchange between the scapolite and the hydrothermal fluid. This comparison allows for a discussion on the potential isotopic exchange scapolite-hydrothermal fluid.

The fluid inclusion leachate and the scapolite pyrohydrolysis solution for sample PAH88217 were measured in different laboratories at different times. However, a comparison between these two phases is plausible given that the fluid inclusion leachates, the pyrohydrolysis solutions and SMOC all have similar matrixes. Also, the Cl in all these solutions was precipitated as AgCl and then converted to CH_3Cl gas following the same methods in both laboratories. Therefore, a significant matrix effect during the IRMS analysis is unlikely. In addition, it has been demonstrated that SMOC can be used as a reference standard (Godon et al., 2004) and in this case, SMOC was used to anchor the isotopic compositions of the hydrothermal fluid and the scapolite in both laboratories.

Although the salinity sources of the Norrbotten scapolites are diverse, as explained above, fluid inclusion analysis of sample PAH88217 suggest a magmatic origin (Gleeson and Smith, 2009 and references there in). In sample PAH88217, the fluid inclusions yielded a $\delta^{37}Cl$ value of -1.7‰ (Gleeson and Smith, 2009) and the scapolite (sample MB02, this study) yielded a value of +0.2‰ (Table 4). From these two values it is possible to calculate a scapolite fluid Cl -isotope fractionation factor ($\Delta^{37}Cl_{scp-fluid}$) of +1.9‰ at temperatures above 500 °C, as proposed by Gleeson and Smith (2009). Although the two minerals are in textural equilibrium (Fig. 10), we are making the assumption that the analyzed fluid in the fluid inclusions was in isotopic equilibrium with the scapolite. To assess the validity of this fractionation factor, we have used a Rayleigh fractionation model to determine if the low $\delta^{37}Cl$ values measured by Gleeson and Smith (2009) can be reproduced.

The Cl isotope co-evolution of fluid and scapolite can be described by a Rayleigh fractionation model (Fig. 10) using an equation adapted from Faure (1986):

$$\delta^{37}Cl_{fluid} = (1000 + \delta^{37}Cl_{o\text{-}fluid}) * F^{(\alpha-1)} - 1000 \quad (1)$$

where $\delta^{37}Cl_{o\text{-}fluid}$ and $\delta^{37}Cl_{fluid}$ are the initial and final isotopic compositions of the hydrothermal fluid, respectively; F is the fraction of Cl left in the hydrothermal fluid after isotope fractionation between the scapolite and the hydrothermal fluid, and α is the observed isotope fractionation factor at a given temperature. Work by Sharp et al. (2007; 2013) suggests a $\delta^{37}Cl$ value of the upper mantle of -1.0 to +0.4‰, averaging -0.3‰. Although others have suggested a lower value (≤ -1.6‰) (Bonifacie et al., 2008), we use a value of -0.3‰ based on the arguments outlined in Sharp et al. (2013). The Rayleigh distillation model (Fig. 10) uses the average mantle values of -0.3‰ for the initial composition of the fluid ($\delta^{37}Cl_{o\text{-}fluid}$). As depicted in Fig. 10, we obtained several curves representing the isotope fractionation and the progressive decrease of Cl in the hydrothermal fluid as consequence of Cl uptake by the mineral phase. For comparison, the isotope fractionation coefficients used in our study and those reported in Kusebauch et al. (2015) for the Bamble scapolites were modeled. Although the isotope fractionation coefficients considered by Kusebauch et al. (2015) reproduced upper mantle values by using the published values for the mantle as the isotopic composition of the initial fluid, the Rayleigh fractionation model applying the empirical +1.9‰ isotope fractionation value, is the only one that reproduces the lowest fluid inclusion $\delta^{37}Cl$ values measured in the set of samples reported in Gleeson and Smith (2009).

This large empirical fractionation factor between scapolite and fluid is not supported by the predictions for monovalent chlorides proposed by Schauble et al. (2003). According to these theoretical calculations, in the case of the scapolites, small isotope fractionations should be expected between a brine with high NaCl activity and scapolite at equilibrium, between 0.37 and 0.68‰ at temperatures from 300 to 600 °C. Theoretical predictions by Schauble et al. (2003) were confirmed by Kusebauch et al. (2015) in scapolites from the Bamble Sector, SE Norway.

However, the fractionation coefficients used by Kusebauch et al. (2015) (1.0005, 1.0007 and 1.0010) to model the Rayleigh fractionation of the hydrothermal fluid at Bamble, cannot produce the low $\delta^{37}Cl$ values measured in the fluid inclusions (Fig. 10).

There are some differences between the scapolites from Norrbotten and the Bamble Sector. For instance, the Norrbotten scapolites are marialites, whereas the Bamble scapolites vary from meionite to marialite. This compositional difference may reflect different sources of salinity and water-rock interaction histories. According to Kusebauch et al. (2015), the Cl identified in the Bamble scapolites has a marine pore fluid origin. This contrasts with the Norrbotten scapolites, which contain Cl from diverse sources (Gleeson and Smith, 2009; this study). Also, at the Pahtohavare deposit, other Cl minerals such as amphibole and biotite have low Cl contents, well below 1 wt% (Alain, 2014), which contrasts with higher Cl contents reported in these minerals by Kusebauch et al. (2015) for the Bamble Sector. Furthermore, in our study, the scapolite formation is associated with $CaCl_2$-rich and CO_2-bearing fluids (Smith et al. 2009), versus the high Na^+, Cl^- and CO_2 fluids identified in the Bamble scapolites (Kusebauch et al. 2015).

Unfortunately, the theoretical isotope fractionation estimates by Schauble et al. (2003) do not include $CaCl_2$-rich brines. Nonetheless, assuming equilibrium, the observed isotope fractionation (+1.9‰) indicates that ^{37}Cl was preferentially accommodated in the A site of the scapolite structure. This suggests that the stable Cl isotope partitioning between the $CaCl_2$-rich brine and the scapolite may be different to the estimates for NaCl brines in equilibrium with silicate minerals considered by Schauble et al. (2003).

It is possible, however, that the relatively high empirical fractionation factor obtained here indicates that fluid and mineral were not in isotopic equilibrium and therefore the values from the Norrbotten scapolites may reflect a kinetic isotope fractionation process. However, isotopic

equilibrium is supported by data from other samples in this study. For example, high $\delta^{37}Cl$ values were found in scapolites from two locations, Pahtohavare (+1.0‰) and Sarkivaara (+0.9‰) (Table 4). The Pahtohavare and Sarkivaara samples have Cl/Br molar ratios of 554 and 271, respectively, which are consistent with typical Cl/Br molar ratios for evaporitic brines. If we use the inferred fractionation factor (+1.9‰) the calculated $\delta^{37}Cl$ value for the hydrothermal fluid is around -1.0‰, consistent with a residual brine (Fig. 8).

If the scapolite investigated in the present study and the hydrothermal fluid did not reach isotopic equilibrium, the low $\delta^{37}Cl$ values identified in fluid inclusions by Gleeson and Smith (2009) must be explained by some other process. These may include water-rock interaction, kinetic isotope fractionation or an unknown source of Cl. None of these options can be assessed in light of the lack of experimental data that quantify the behavior of the stable Cl isotopes during water-rock interaction. Future work should focus on fractionation experiments. However, at the present time the most parsimonious interpretation is that low $\delta^{37}Cl$ values seen in fluid inclusions formed as a result of the preferential uptake of ^{37}Cl into a mineral reservoir represented by scapolite, and possible other silicate minerals.

6. Conclusions

The scapolites investigated from the Norrbotten County have a predominantly marialitic composition. Some chemical variations are present, particularly in samples from IOCG-PS alteration, which are more Ca and S enriched and Na and Cl depleted than the other two alteration types. In contrast, IOCG-M scapolites are more Cl and Fe rich, but depleted in Ca. The RM scapolites have intermediate compositions. In addition, relative SO_4-Cl-CO_3 compositions and temporal correlations suggest that RM scapolites may have been incorporated or recycled into the later IOCG alteration. This is also confirmed by the halogen compositions of Kallosalmi,

Gruvberget, Pahtohavare, Nunasvaara and Torneälven scapolites. Some scapolite samples from Pahtohavare and the sample from the Sarkivaara deposit contain lower than seawater Cl/Br molar ratios (554 and 271), indicating the presence of evaporative residual brines. All the other scapolites have halogen signatures related to seawater, magmatic and evaporitic sources (halite and residual brines).

Measured $\delta^{37}Cl$ values in fluid inclusions (Gleeson and Smith, 2009) and spatially related scapolite in one of the samples allowed the calculation of an empirical isotope fractionation of +1.9‰ between the mineral and the fluid. This value contradicts predictions for isotope fractionation between a silicate mineral such as scapolite and a monovalent hydrothermal fluid with high NaCl activities. However, using a Rayleigh fractionation model starting with upper mantle values, we reproduced the lowest $\delta^{37}Cl$ values reported by Gleeson and Smith (2009) in fluid inclusions from deposits of the Norrbotten County. Conversely, if the scapolite investigated in the present study and the hydrothermal fluid did not reach isotopic equilibrium, the low $\delta^{37}Cl$ values identified in fluid inclusions by Gleeson and Smith (2009) must be explained by some other process, which may include water-rock interaction, kinetic isotope fractionation or an unknown source depleted in ^{37}Cl. Our results suggest that more experimental data on fractionation factors for the scapolite-hydrothermal brine system are needed to test the theoretical predictions proposed by Schauble et al. (2003).

The complex geologic history of the Norrbotten district is reflected in the chemical and isotopic composition of its mineral alteration. Owing to the persistence of regional metamorphism and the recurrence of magmatic episodes, the hydrothermal fluids contain both recycled and new components that formed the proximal scapolites. Although halogen compositions of IOCG alteration appear more representative of the original hydrothermal fluids, more research has to be

done to better understand the evolution of the Cl isotopes in RM scapolites, and the extent of the Cl isotopic fractionation at high temperatures between hydrothermal fluids and Cl-bearing minerals.

7. Acknowledgements

This study was funded with a NSERC Discovery grant to S.A. Gleeson. The authors thank Tom Chacko for his helpful comments. We also thank Jake Hanley for providing the internal biotite standard used to stablish the efficiency of the pyrohydrolysis extraction method. We also thank two anonymous reviewers for helpful comments and David Hilton for editorial handling.

Fig. 1. Location of the Norrbotten district, North Sweden. Geology from Bergman et al. (2001).

Fig. 2. Field context of scapolitisation at Norrbotten. (A) Altered scapolite and greenschist facies metabasites at Torneälven River showing, scapolite veins with actinolite selvedges cutting the outcrop (RM). (B) Well preserved greenschist facies pillow breccia at Torneälven River. The matrix is intensely scapolite-albite altered. Note the pillow breccias and clasts also pervasively altered with actinolite on margins (RM). (C) Scapolite-altered diorite at Nunasvaara (RM). (D) Scapolite-albite altered metasediment in breccia. Note sedimentary laminations still preserved. Actinolite matrix (RM). (E) Scapolite alteration in greenschist facies of dolerite dyke rock at Pahtohavare (IOCG-M). (F) Magnetite-actinolite-calcite vein cutting intensely Na-altered metavolcanic rock at Gruvberget (IOCG-PS).

Fig. 3. Representative textures in scapolite. (A) 04Torn1 – Scapolite in greenschist facies pillow basalt (RM). (B) 04Torn1 – Scapolite-actinolite-chlorite vein in metabasalt. (C) N3.4D - Scapolite replacing plagioclase in meta-diorite (RM). (D) PAH88097 33.95m – Scapolite-

actinolite-biotite alteration of dolerite dyke (IOCG-M). (E) PAH88093 19.35m – Scapolite metasomatite associated with chalcopyrite mineralisation (IOCG-PS). (F) SAR1 – Scapolite metasomatite ('Na-skarn') associated with chalcopyrite and molybdenite mineralisation (IOCG-PS). Act- actinolite; Scp – Scapolite; Ttn – Titanite; Plg – Plagioclase; Mgt – Magnetite; Chl – Chlorite; Bt – Biotite; Py – Pyrite; Cpy – Chalcopyrite.

Fig. 4. Schematic diagram of the pyrohydrolysis apparatus used to extract Cl from scapolites.

Fig. 5. Distribution of major ions in scapolites. A) Cl vs. Ca/(Na+K+Ca) (a.p.f.u.). B) Fe-S-K. Regional Na-Cl metasomatism (RM) alteration, IOCG-Scapolite altered metabasites (IOCG-M) and IOCG-Proximal Scapolite-rich alteration/Na-Skarn (IOCG-PS).

Fig. 6. A. Ternary diagram SO_4-Cl-CO_3. Relative anion contents of scapolites in atomic proportions from formulae calculated assuming 12 (Si, Al). Carbonate was calculated by difference assuming a full anion site occupancy. B. Ternary diagram SO_4-Cl-CO_3 showing individual analysis in scapolite grains. IOCG deposits: IOCG-PS and IOCG-M. Fields are made of individual EPMA points (Table 3).

Fig. 7. Halogen compositions: Cl/Br molar ratios vs Br concentrations. Regional Na-Cl Metasomatism alteration (RM), IOCG-scapolite altered metabasites (IOCG-M) and IOCG-proximal scapolite-rich alteration/Na-Skarn (IOCG-PS). Fluid inclusion data from Gleeson and Smith (2009). MSW: modern seawater.

Fig. 8. δ^{37}Cl values vs. Cl/Br molar ratios of scapolites. Data includes regional Na-Cl metasomatism (RM) alteration, IOCG-Scapolite altered metabasites (IOCG-M) and IOCG-Proximal Scapolite-rich alteration/Na-Skarn (IOCG-PS) samples. Cl/Br molar ratios and δ^{37}Cl values for magmatic sources from Jambon et al., (1995); Johnson et al., (2000); Sharp et al.,

(2007), Nahnybida et al., (2009) and Gleeson and Smith (2009). Evaporite values from Eastoe et al. (2007). Halite Cl/Br molar ratios from Eggenkamp et al., (1995), Eastoe et al. (1999), Eastoe and Peryt, (1999), Peryt et al., (2005) and Eastoe et al. (2007).

Fig. 9. (Top) PAH88217 18.20m – Scapolite metabasite, Pahtohavare (IOCG-M). (Bottom) PAH88097 33.95m – Scapolite-actinolite-quartz-biotite alteration of dolerite dyke (IOCG-M).

Fig. 10. Rayleigh fractionation curves. Evolution of the fluid using the equation: $\delta^{37}Cl_{fluid}=(1000+\delta^{37}Cl_{o\text{-}fluid})*F^{(\alpha-1)}$ -1000 (adapted from Faure, 1986). Where, $\delta^{37}Cl_{o\text{-}fluid}$ and $\delta^{37}Cl_{fluid}$ are the initial and final isotopic compositions of the hydrothermal fluid, respectively; F is the fraction of Cl left in the hydrothermal fluid after isotope fractionation between the scapolite and the hydrothermal fluid, and α is the observed isotope fractionation factor at a given temperature. Using this equation starting with an initial upper mantle $\delta^{37}Cl$ value of -0.3‰ (Sharp et al. 2013), hydrothermal fluid values identified by Gleeson and Smith (2009) are reproduced.

Table 1. Summary of pyrohydrolysis results. Mineral composition of sample separates, size fractions, scapolite grains, Cl content of each sample and description of the pyrohydrolysis solution: volume recovered, Cl concentration and yield.

Table 2. Efficiency of the pyrohydrolysis method using the internal biotite standard.

Table 3. Average major oxide compositions by microprobe in scapolite samples. Formula calculations assuming 12 (Al, Si), carbonate calculated by difference assuming a full anion site occupancy.

Table 4. Scapolite analysis results. Cl, Br and Na composition of scapolite samples by microprobe and XRFM analysis, and stable Cl isotopes.

8. References

Alain V. 2014. Mineral chemistry and texture paragenesis of alteration minerals in the Patohavare Cu-Au deposit, Sweden. Master's Thesis. Luleå university of Technology.

Barnes, J.D., and Sharp, Z.D., 2006. A chlorine isotope study of DSDP/ODP serpentinized ultramafic rocks: insights into the serpentinization process. Chem. Geol. 228, 246- 265.

Barton M. D. and Johnson D. A., 1996. Evaporitic-source model for igneous-related Fe oxide-(REE–Cu–Au–U) mineralisation. Geology 24, 259–262.

Barton, M. D. & Johnson, D. A., 2000. Alternative brine sources for Fe-oxide Cu-Au systems: Implications for hydrothermal alteration and metals. In: Porter, T. M. (ed.) Hydrothermal Iron Oxide Copper-Gold and Related Deposits: A Global Perspective. Adelaide: Austra. Min. Foun., 43-60.

Benavides J., Kyser T., Clark A., Oates C., Zamora, R. Tarnovschi R., Castillo B., 2007. The Mantoverde iron oxide-copper-gold district, III region, Chile; the role of regionally derived, nonmagmatic fluids in chalcopyrite mineralisation. Econ. Geol. 102, 415-440.

Bergman S., Ku¨ bler L. and Martinsson O., 2001. Description of the Regional Geological and Geophysical Maps of Northern Norrbotten County (East of the Caledonian Orogen). Geological Survey of Sweden (Sveriges Geologiska Underso¨kning). Ba56, 110.

Billström K. and Martinsson O., 2000. Links between epigenetic Cu–Au mineralisations and magmatism/deformation in the Norrbotten County, Sweden. In: 2nd GEODE Fennoscandian Shield Field Workshop on Palaeoproterozoic and Archaean Greenstone Belts and VMS Districts in the Fennoscandian Shield, Lulea University of Technology, Research Report 06, p. 6.

Bonifacie M., Jendrzejewski N., Agrinier P., Coleman M., Pineau F. and Javoy M., 2007. Pyrohydrolysis-IRMS determination of silicate chlorine stable isotope compositions. Application to oceanic crust and meteorite samples. Chem. Geol. 242, 187-201.

Bonifacie, M., Jendrzejewski, N., Agrinier, P., Humler, E., Coleman, M., and Javoy, M., 2008. The chlorine isotope composition of Earth's mantle: Science 359, 1518–1520.

Böhlke J. and Irwin J., 1992. Laser microprobe analyses of Cl, Br, I, and K in fluid inclusions: implications of sources in some ancient hydrothermal fluids. Geochim. et Cosmochim. Acta 56, 203-225.

Chen H., Clark A. and Kyser K., 2010. The Marcona magnetite deposit, Ica, south-central Peru: A product of hydrous, iron-oxide-rich melts?. Soc. Econ. Geol. 105, 1441-1456.

Chiaradia M., Banks D. A., Cliff R., Marschik R. and de Haller A., 2006. Origin of fluids in iron oxide–copper–gold deposits: constraints from $\delta^{37}Cl$, Sr^{87}/Sr^{86} and Cl/Br. Min. Dep. 41, 565–573.

Corriveau L., 2007. Iron oxide copper-gold deposits: a Canadian perspective. Mineral Deposits of Canada: a Synthesis of Major Deposit-Types, District Metallogeny, the Evolution of Geological Provinces and Exploration Methods. Geol. Asso. Can. Min. Dep. Div., Spe. Vol. 5, 307-328.

Dong P., 2005. Halogen-element (F, Cl and Br) behaviour in apatites, scapolite, and sodalite: an experimental investigation with field applications. Thesis. Department of Geological Sciences. University of Saskatchewan. 234p.

Eastoe, C.J., Peryt, T., 1999. Multiple sources of chloride in Badenian evaporites, Carpathian Mountains: stable chlorine isotope evidence. Terra Nova 11, 118–123.

Eastoe, C.J., Long, A., Knauth, L.P., 1999. Stable chlorine isotopes in the Palo Duro Basin, Texas: evidence of preservation of Permian evaporite brines. Geochim. Cosmochim. Acta 63, 1375–1382.

Eastoe, C.J., Peryt, T.M., Petrychenko, O.Y., Geisler-Cussey, D., 2007. Stable chlorine isotopes in Phanerozoic evaporites. Appl. Geochem. 22, 575–588. Edfelt, Å. Armstrong, R. N., Smith, M. P. & Martinsson, O., 2005. Alteration aragenesis and mineral chemistry of the Tjärrojäkka apatite-iron and Cu (-Au) occurrences, Kiruna area, northern Sweden. Mineral. Dep. 40, 409-434.

Eggenkamp, H.G.M., Kreulen, M.R., Koster Van Groos, A.F., 1995. Chlorine stable isotope fractionation in evaporites. Geochim. Cosmochim. Acta 59, 5169–5175.

Ellis D., 1978. Stability and phase equilibria of chloride and carbonate bearing scapolite at 750 and 400 bar. Geochim. et Cosmochim. Acta. 42, 1271-1281.

Faure G., 1986. Principles of Isotope Geology. second ed. J.Wiley and Sons, p. 589.

Fisher L. A. and Kendrick M. A., 2008. Metamorphic fluid origins in the Osborne Fe oxide–Cu–Au deposit, Australia: evidence from noble gases and halogens. Min. Dep. 43, 483–497.

Frietsch, R., Tuisku, P., Martinsson, O. & Perdahl, J. A. 1997. Early Proterozoic Cu-(Au) and Fe ore deposits associated with regional Na-Cl metasomatism in northern Fennoscandia. Ore Geol. Rev. 12, 1-34.

Gleeson S. A. 2003. Bulk analysis of electrolytes in fluid inclusions. Fluid inclusions: Analysis and interpretation, Short course series 32, 233-246.

Gleeson, S.A., and Smith, M.P., 2009. The sources and evolution of mineralising fluids in Fe oxide-apatite and iron oxide-copper-gold systems, Norrbotten, Sweden: Constraints from stable Cl isotopes of fluid inclusion leachates. Geochim. et Cosmochim. Acta 73, 5658-5672.

Gleeson S.A., Turner W.A., 2007. Fluid inclusion constraints on the origin of the brines responsible for Pb-Zn mineralisation at Pine Point and coarse non-saddle and saddle dolomite formation in southern Northwest Territories. Geofluids 7, 51–68.

Godon, A., Jendrzejewski, N., Eggenkamp, H.G.M., Banks, D.A., Ader, M., Coleman, M.L., Pineau, F., 2004. A cross calibration of chlorine isotopic measurements and suitability of seawater as the international reference material. Chem. Geol. 207, 1–12.

Govindaraju K., 1994. 1994 compilation of working values and sample description for 383 geostandards. Geostandards Newslett. 18.

Hammerli J, Rusk B, Spandler C, Emsbo P, Oliver N.H.S., 2013. In situ quantification of Br and Cl in minerals and fluid inclusions by LA-ICP-MS: A powerful tool to identify fluid sources. Chem. Geol. 337-338, 75-87.

Jambon A., De´ruelle B., Dreibus G. and Pineau F., 1995. Chlorine and bromine abundance in MORB: the constrasting behaviour of the Mid-Atlantic Ridge and East Pacific Rise and implications for chlorine geodynamic cycle. Chem. Geol. 126, 101–117.

Johnson L. H., Burgess R., Turner G., Milledge J. H. and Harris J. W., 2000. Noble gas and halogen geochemistry of mantle fluids: comparison of African and Canadian diamonds. Geochim et Cosmochim. Acta 64, 717–732.

Kendrick M. A., Burgess R., Patrick R. A. D. and Turner G., 2001. Fluid inclusion noble gas and halogen evidence on the origin of Cu-Porphyry mineralising fluids. Geochim. et Cosmochim. Acta 65, 2651-2668.

Kendrick M. A., Mark G. and Phillips D., 2007. Mid-crustal fluid mixing in a Proterozoic Fe oxide–Cu–Au deposit, Ernest Henry, Australia: evidence from Ar, Kr, Xe, Cl, Br, and I. Earth Planet. Sci. Lett. 256, 328–343.

Kendrick M. A., Honda M., Gillen D., Baker T. and Phillips D., 2008a. New constraints on regional brecciation in the Wernecke Mountains, Canada from He, Ne, Ar, Kr, Xe, Cl, Br and I in fluid inclusions. Chem. Geol. 255, 33–36.

Kendrick M. A., Baker T., Fu B., Phillips D. and Williams P. J., 2008b. Noble gas and halogen constraints on regionally extensive mid-crustal Na–Ca metasomatism, the Proterozoic Eastern Mount Isa Block, Australia. Precambrian Res. 163, 131–150.

Kendrick M. A., Kamenetsky V. S., Phillips D. and Honda M., 2012, Halogen systematics (Cl, Br, I) in Mid-Ocena Ridge Basalt: a Macquarie Island case study. Geochim. et Cosmochim. Acta 81, 82-93.

Kesler S. E., Appold M. S., Martini A. M., Walter L. M., Huston T. J. and Kyle J. R., 1995. Na–Cl–Br systematics of mineralising brines in Mississippi Valley-type deposits. Geology 23, 641–644.

Kusebauch C., John T., Barnes J. and Klügel A and Austrheim H., 2015. Halogen element and stable chlorine isotope fractionation caused by fluid–rock interaction (Bamble Sector, SE Norway). Jour. Petrol. doi:10.1093/petrology/egv001.

Lindblom, S., Broman, C. & Martinsson, O., 1996. Magmatic-hydrothermal fluids in the Pahtohavare Cu-Au deposit in greenstone at Kiruna, Sweden. Min. Dep. 31, 307-318.

Martinsson, O., 1997.Tectonic setting and Metallogeny of the Kiruna Greenstones. Doctoral thesis, Lule University of Technology.

Martinsson, O., 2004. Geology and Metallogeny of the Northern Norrbotten Fe^Cu^Au Province. In: Allen, R. L., Martinsson, O. & Weihed, P. (eds) Svecofennian Ore-Forming Environments: Volcanic-Associated Zn-Cu-Au-Ag, Intrusion-Associated Cu-Au, Sediment-Hosted Pb-Zn, and Magnetite-Apatite Deposits of Northern Sweden, Soc. Econ. Geol. Guidebook Series 33, 131-148.

Martinsson, O. and Virkkunen, R., 2004. Apatite Iron Ores in the Gällivare, Svappavaara, and Jukkasjä rvi Areas. In: Allen, R. L., Martinsson, O. & Weihed, P. (eds) Svecofennian Ore-Forming Environments: Volcanic-Associated Zn-Cu-Au-Ag, Intrusion-Associated Cu-Au, Sediment-Hosted Pb-Zn, and Magnetite-Apatite Deposits of Northern Sweden, Soc. Econ. Geol. Guidebook Series 33,167-172.

Mi, J.-X. and Pan, Y. 2016. Halogen-rich minerals: Crystal chemistry and geological significances. In: Harlov, D. (ed) Role of Halogens in Terrestrial and Extraterrestrial Processes, Springer (invited contribution; publication expected in the fall of 2016).

Mora, C.I. and Valley, J.W., 1989. Halogen-rich scapolite and biotite: Implications for metamorphic fluid-rock interaction. The Amer. Mineral. 74, 721-737.

Nahnybida T., Gleeson S.A, Rusk B. and Wassenaar L., 2009. Cl/Br ratios and stable chlorine isotope analysis of magmatic-hydrothermal fluid inclusions from Butte, Montana and Bingham Canyon, Utah. Miner. Deposita 44, 837-848.

Oliver, N. H. S., Cleverley, J. S., Mark, G., Pollard, P. J., Bin Fu, , Marshall, L. J., Rubenach, M. J., Williams, P. J. & Baker, T., 2004. Modeling the role of sodic alteration in the genesis of iron oxide-copper-gold deposits, eastern Mount Isa block, Australia. Econ. Geol. 99, 1145-1176.

Orville M. P., 1975. Stability of scapolite in the system Ab-An-NaCl-$CaCO_3$ at 4kb and 750ºC. Geochim. et Cosmochim. Acta. 39, 1091-1105.

Pan Y. and Dong P., 2003. Bromide in scapolite-group minerals and sodalite: XRF microprobe analysis, exchange experiments, and application to skarn deposits. The Can. Mineral. 41, 559-540.

Peryt, T.M., Tomassi-Morawiec, H., Czapowski, G., Hryniv, S.P., Pueyo, J.J., Eastoe, C.J., Vovnyuk, S., 2005. Polyhalite occurrence in the Werra (Zechstein, Upper Permian) Peribaltic Basin of Poland and Russia: evaporite facies constraints. Carbonat. Evapor. 20, 182–194.

Pollard P. J., 2000. Evidence of a magmatic fluid and metal source for Fe-oxide Cu–Au mineralisation. In Hydrothermal Iron Oxide Copper–Gold and Related Deposits: A Global Perspective (ed. T. M. Porter). Austral. Mineral Found. 27–41.

Pollard P. J., 2006. An intrusion-related origin for Cu–Au mineralisation in iron oxide–copper–gold (IOGC) provinces. Min. Dep. 41, 179–197.

Romer R.L., Kjösnes B., Korneliussen A., Lindah, I., Skysseth T., Stendal, H. & Sundvoll B, 1992. The Archaean-Proterozoic boundary beneath the Caledonides of northern Norway and Sweden: U-Pb, Rb-Sr and Nd isotopic data from the Rombak-Tysfjord area: Norges Geologiske Undersøkelse, Rapport 91, 225, 67 p.

Romer, R.L., Martinsson, O., and Perdahl, J.-A., 1994. Geochronology of the Kiruna iron ores and hydrothermal alterations: Econ. Geol. 89, 1249–1261.

Sanjuan B., Michard G., Michard A., 1990. Origine des substances dissoutes das les eaux des sources thermals et des forages de la région Asal Ghoubbet (République de Djibouti). J. Volcanol. Geoth. Res 43,333-352.

Schauble E., Rossman G. and Taylor H., 2003. Theoretical estimates of equilibrium chlorine-isotope fractionations. Geochim. et Cosmochim. Acta. 67. 17: 3267-3281.

Sharp Z., Barnes J., Brearley A., Chaussidon M., Fischer T. and Kamenetsky V., 2007. Chlorine isotope homogeneity of the mantle, crust and carbonaceous chondrites. Nature, Lett. 446, nature05748.

Sharp Z., Mercer J., Jones R., Brearley A., Selverstone J., Bekker A., and Stachel T., 2013. The chlorine isotope composition of chondrites and Earth. Geochim. et Comochim. Acta. 107, 189-204.

Smith, M. P., Coppard, J., Herrington, R. & Stein, H., 2007. The geology of the Rakkurijärvi Cu-(Au) prospect, Norrbotten: A new IOCG deposit in Northern Sweden. Econ. Geol. 102, 393-414.

Smith, M.P., Storey, C.D., Jeffries, T.E., and Ryan, C., 2009. In Situ U-Pb andTrace Element Analysis of Accessory Minerals in the Kiruna District, Norrbotten, Sweden: New Constraints on the Timing and Origin of Mineralisation. J. Petrol. 50, 2063-2094.

Smith M.P., Gleeson S.A., and Yardley B.W.D., 2012. Hydrothermal fluid evolution and metal transport in the Kiruna District, Sweden: Constraining metal behaviour in aqueous and aqueous-carbonic brines. Geochim. et Cosmochim. Acta. 102: 89-112.

Walter, L. M., Stueber, A. M., and Huston, T. J., 1990. Br-Cl-Na systematics in Illinois Basin fluids: Constraints on fluid origin and evolution: Geology 18, 315–318.

Wanhainen C., Broman C., and Marinsson O., 2003. The Aitik Cu-Au-Ag deposit in northern Sweden: a product of high salinity fluids. Min. Dep. 38, 715-726.

Wanhainen C., Broman C., Martinsson O., and Magnor B., 2012. Modification of a paloeproterozoic porphyry-like system: Integration of structural geochemical, petrographic, and fluid inclusion data from the Aitik Cu-Au-Ag deposit, northern Sweden. Ore Geol. Rev. 48, 306-331.

Wägman, K. & Ohlsson, L. G., 2000. Exploration opportunities in Norrbotten: Municipality of Kiruna. Stockholm: Mineral Resources Information Office, Sveriges Geologiska Undersökning, 278 p.

Whitehead D. and Tomas J. E., 1985. Use of a Nebulizer in pyrohydrolytic Decomposition of silicate materials for determination of fluorine and chlorine. Anal. Chem. 57, 2421-2423.

Williams P.J., Barton M.D., Johnson D.A., Fontboté L., de Haller A., Mark G., Oliver N.H.S., Marschik R., 2005. Iron oxide–copper–gold deposits: geology, space–time distribution, and possible modes of origin. In: Hedenquist JW, Thompson JFH, Goldfarb RJ, Richards JP (eds) Econ. Geol. 100 Anniversary Volume, 371–405.

Williams, C.T., 1996. Analysis of rare earth minerals. In: Jones, A. P., Wall, F. & Williams, C. T. (eds) Rare Earth Minerals: Chemistry, Origin and Ore Deposits. London: Chapman & Hall, 327-348.

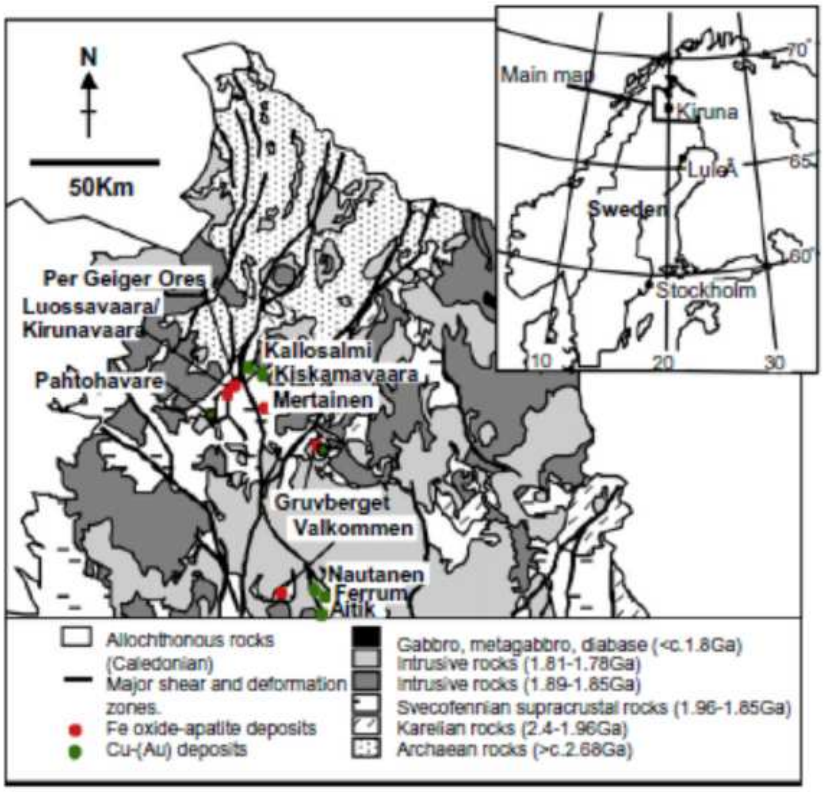

Fig. 1.

Fig. 2.

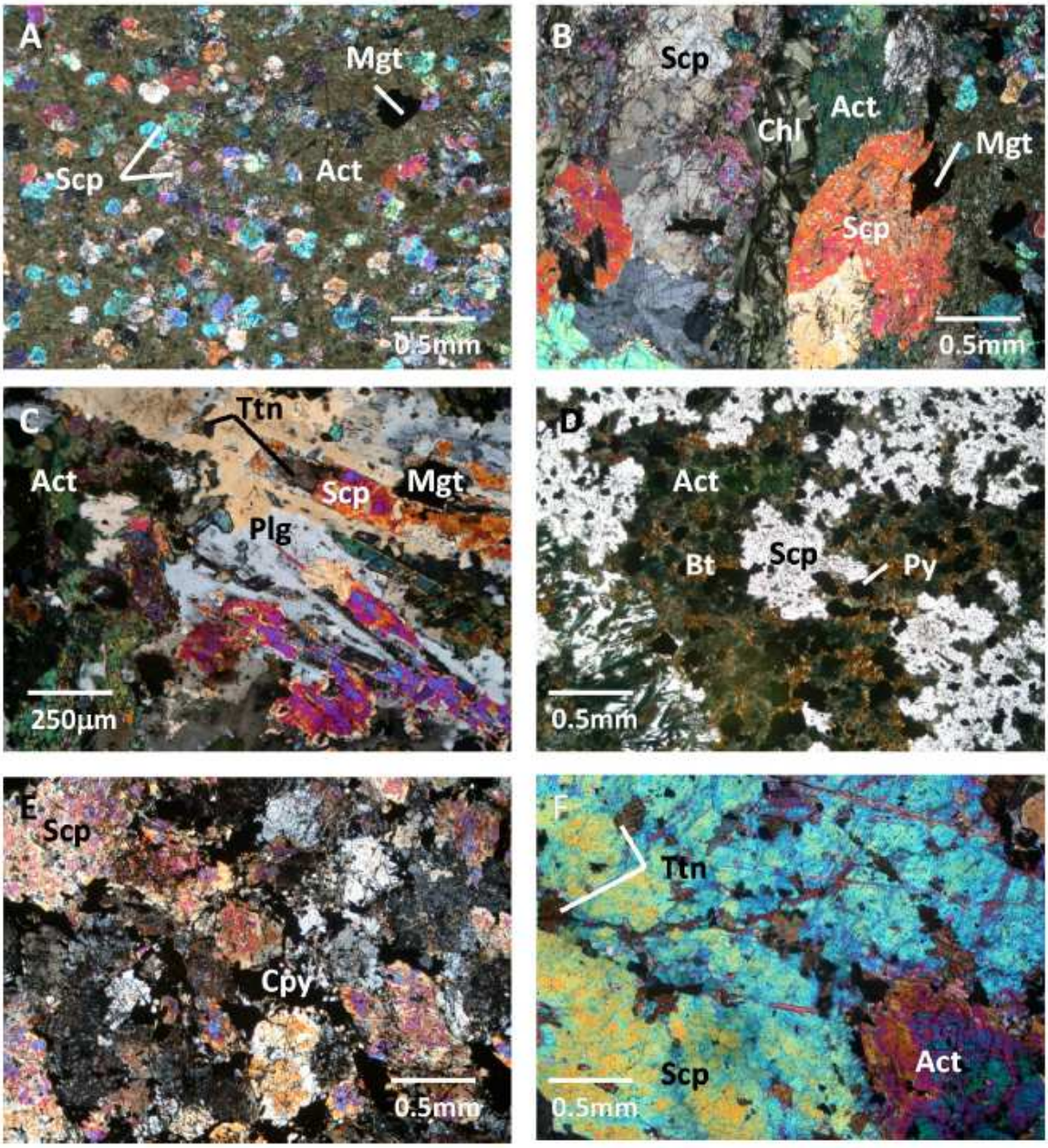

Fig. 3.

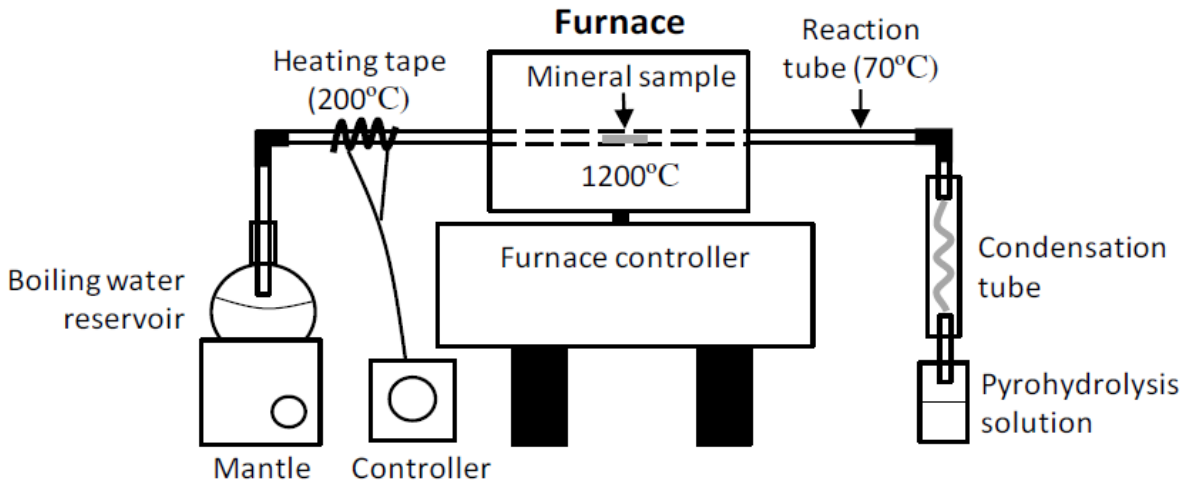

Fig. 4.

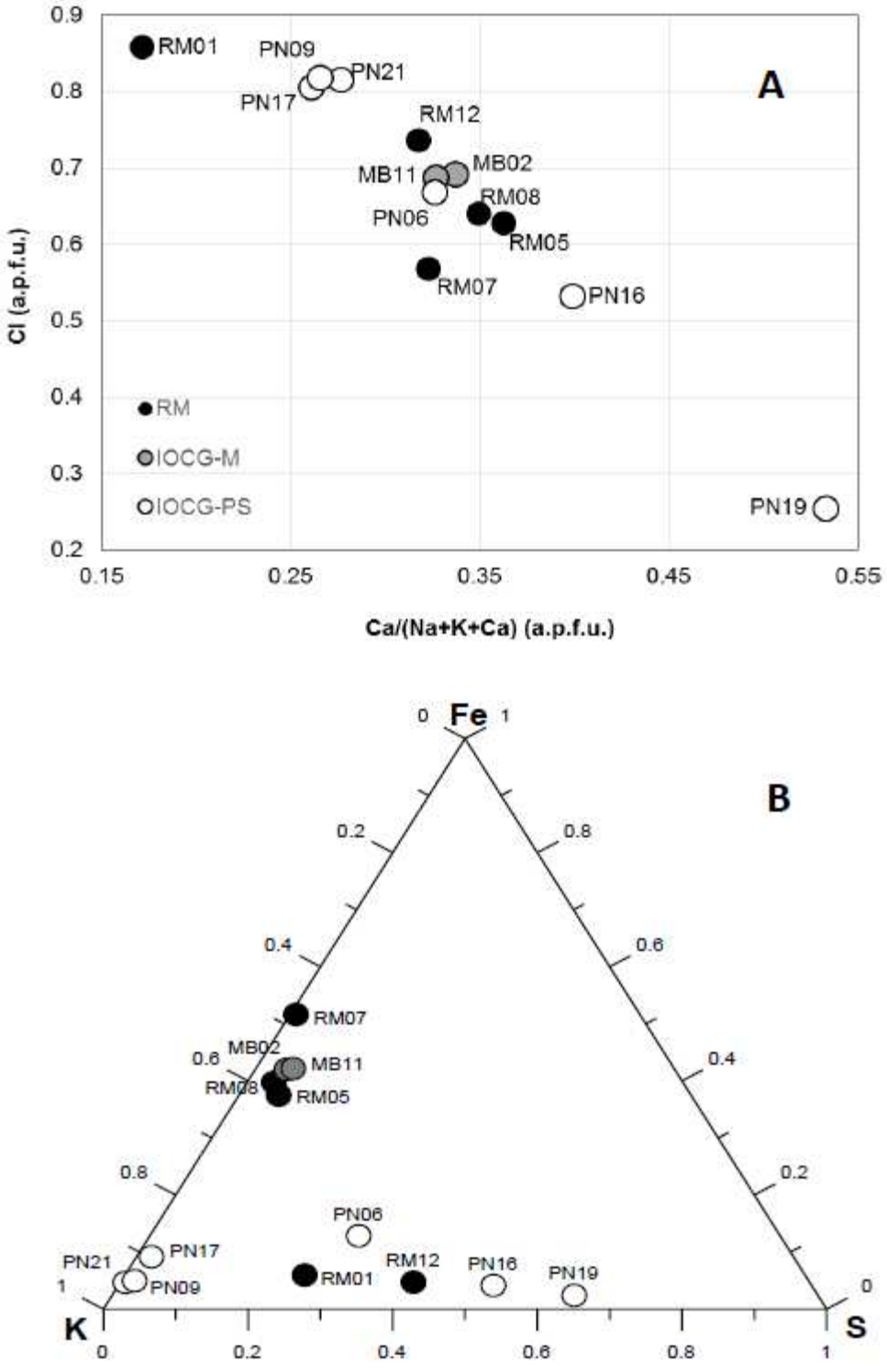

Fig. 5

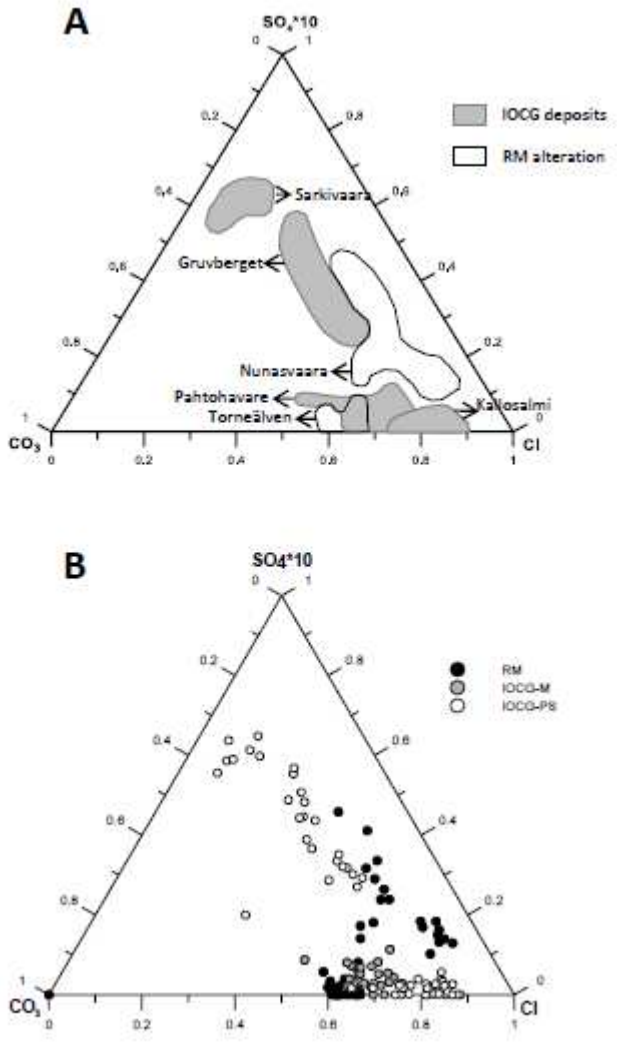

Fig. 6

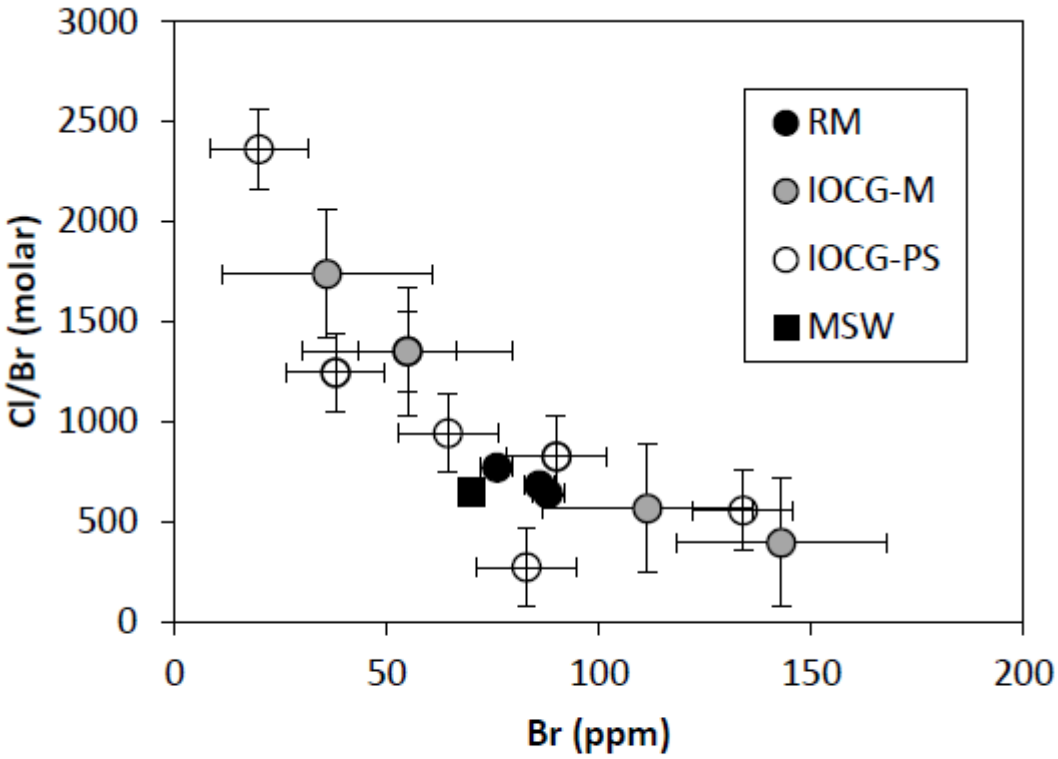

Fig. 7

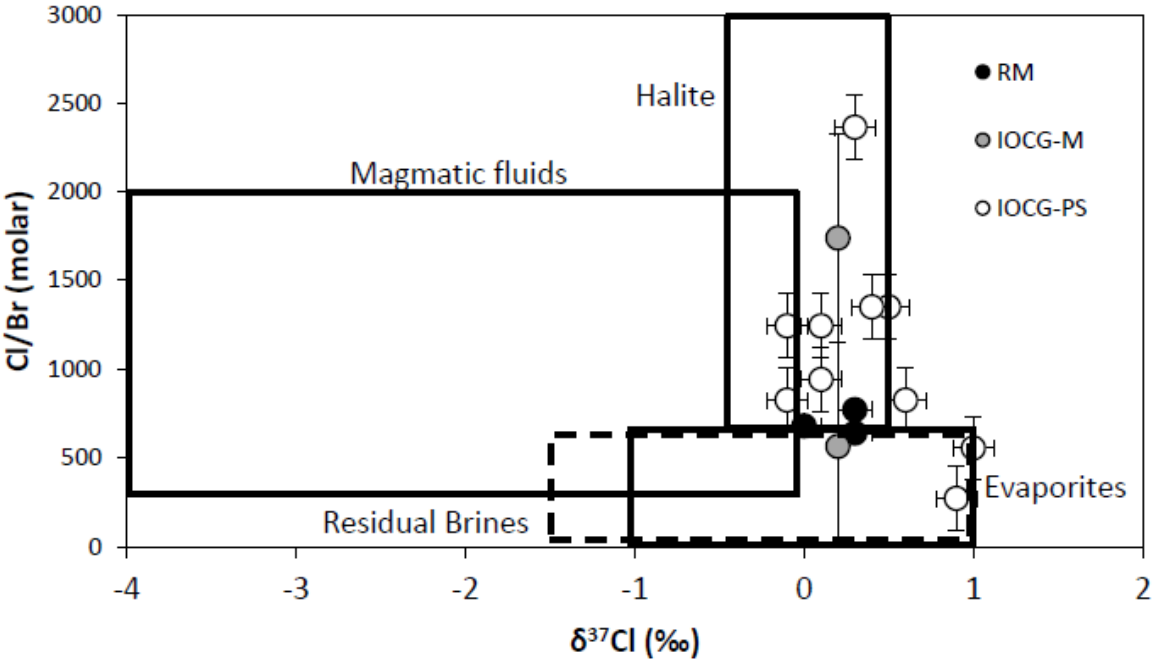

Fig. 8

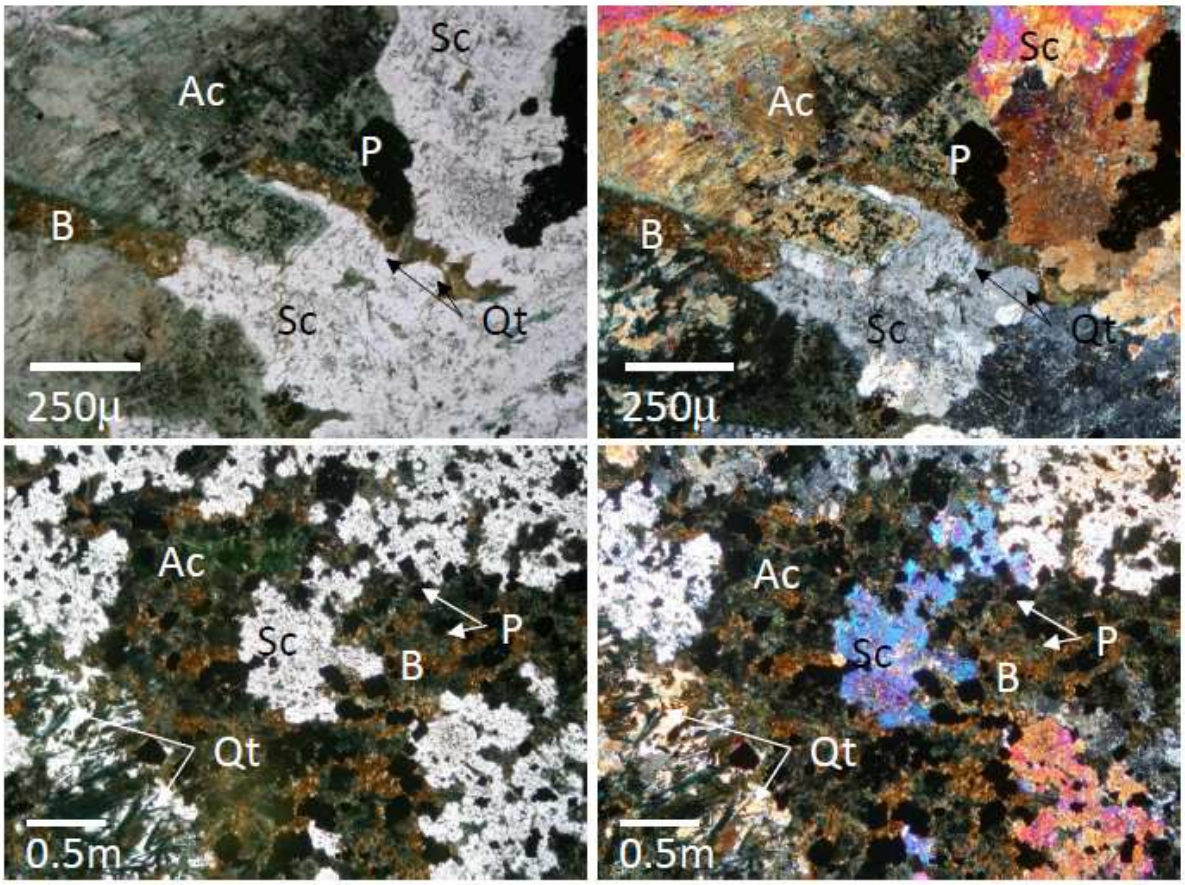

Fig. 9.

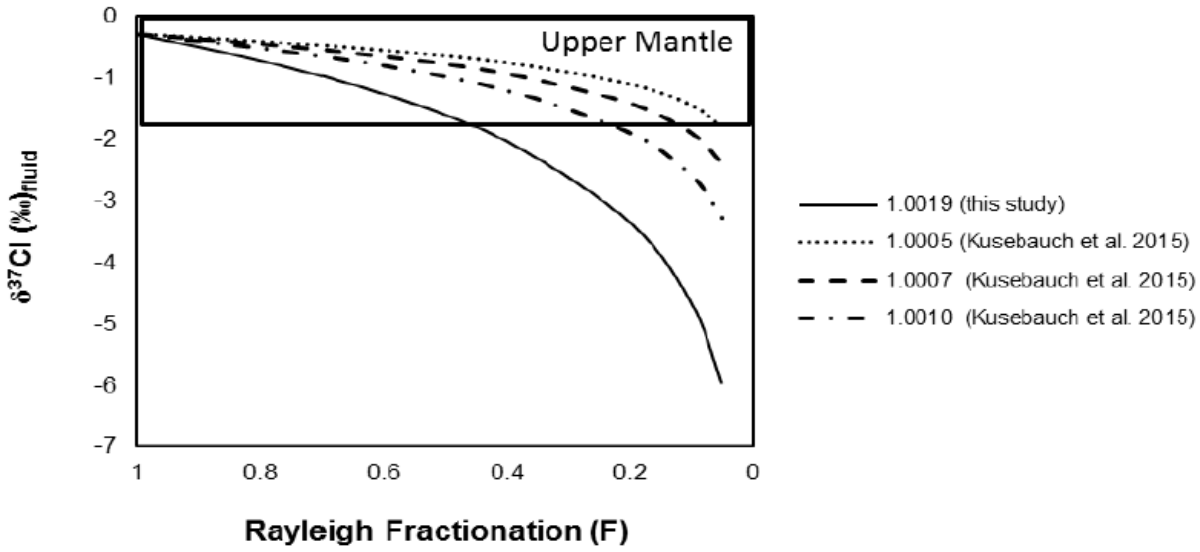

Fig. 10

Table 1

ID	Sample	Minerals by SEM	Mineralization	Sample size fraction (μm)	Scapolite grains %	Cl in Scapolite (mg)	Pyrohydrolysis		
							Solution (mL)	Cl (mg)	Yield %
RM01	03NUN29	Scp, Alb and Ksp	RM	125-250	73	3.18	113	3.84	121
RM13	04TORN1veinwr	Scp	RM	100-125	100	2.45	100	1.80	73
RM07	04 TORN 1 vein	Scp	RM	250-500	100	3.90	134	2.80	72
RM08	04 TORN 1 vein	Scp	RM	125-250	100	3.98	130	2.80	70
RM05	04 TORN 2	Scp	RM	125-250	100	4.00	123	3.97	99
MB02	PAH 88217	Scp	IOCG-M	125-250	100	4.84	118	4.50	93
MB10	03PAH3	Scp	IOCG-M	125-250	100	3.42	90	2.88	84
PN09	KAL 90107 56.38m	Scp	IOCG-PS	125-250	100	4.29	161	3.86	90
PN21	KAL 90106 118.4m	Scp	IOCG-PS	100-125	100	4.82	124	1.16	24
PN20	KAL 90106	Scp	IOCG-PS	125-250	100	4.95	126	1.87	38
PN17	PAH 88093	Scp	IOCG-PS	100-125	100	5.02	103	4.14	83
PN18	PAH 88093	Scp	IOCG-PS	125-250	100	3.76	100	2.93	78
PN16	G1-1	(Alb+An), Qz, Scp, Ksp, Cal	IOCG-PS	100-125	34	1.14	108	1.02	90
PN14	G1-1	(Alb+An), Qz, Scp, Ksp, Cal	IOCG-PS	250-500	34	1.05	100	1.49	142
PN15	G1-1	(Alb+An), Qz, Scp, Ksp, Cal	IOCG-PS	125-250	34	1.12	107	1.25	112
PN06	G4-1	Scp	IOCG-PS	125-250	100	3.38	100	2.63	78
PN19	SAR1	Scp	IOCG-PS	125-250	100	2.26	111	2.05	91

Scp: scapolite, Alb: albite, Ksp: potassium feldspar, An: anorthite, Qz: quartz, Cal: calcite. RM: Regional Alteration Na-Cl Metasomatism, IOCG-M: IOCG-Sc altered Metabasic Rocks, IOCG-PS: IOCG-Proximal sc-rich alt/Na Skarn.

Table 2

Sample	*Cstd (ppm)*	*Mass Measured (g)*	*Cl expect (mg)*	*Cl by IC (ppm)*	*Vol Recov (mL)*	*Cl Recov (mg)*	*Yield %*
Bt1	1900	0.1144	0.2174	1.56	124	0.1934	89
Bt2	1900	0.1009	0.1917	1.49	118	0.1758	92
Bt3	1900	0.1073	0.2039	1.68	115	0.1932	95

Table 3

Sample/analyte wt% oxide	*RM12*	*RM01*	*RM08*	*RM07*	*RM05*	*MB02*	*MB11*	*PN17*	*PN21*	*PN09*	*PN06*	*PN16*	*PN19*
F	n.d.	n.d.	n.d.	n.d.	n.d.	n.d.	n.d.	n.d.	n.d.	n.d.	n.d.	n.d.	n.d.
Na_2O	9.63	11.99	9.27	9.24	9.00	9.36	9.36	10.45	9.59	10.13	9.23	8.29	6.23
MgO	n.d.	0.01	0.09	0.08	0.01	0.12	0.27	n.d.	n.d.	0.01	0.02	n.d.	0.04
Al_2O_3	23.27	21.14	23.41	23.16	23.44	23.22	23.14	21.87	21.83	21.93	22.62	22.99	24.59

SiO_2	55.14	59.08	54.58	55.61	54.41	54.59	55.10	56.82	56.25	56.67	55.56	53.24	50.30
SO_3	0.37	0.17	0.02	n.d.	0.02	0.03	0.06	0.02	0.01	0.02	0.40	0.74	1.05
Cl	3.00	3.56	2.59	2.29	2.54	2.80	2.80	3.29	3.29	3.33	2.71	2.11	1.00
CaO	8.35	4.59	9.15	9.06	9.43	8.83	8.53	6.91	7.23	6.99	8.52	10.43	13.55
K_2O	0.50	0.46	0.26	0.23	0.26	0.38	0.58	0.66	1.34	0.91	0.80	0.62	0.55
FeO*	0.04	0.04	0.18	0.25	0.17	0.30	0.46	0.07	0.07	0.05	0.18	0.06	0.04
Total	100.30	101.05	99.54	99.95	99.28	99.62	100.28	100.08	99.62	100.03	100.02	98.48	97.36
Cl = O	0.68	0.80	0.58	0.52	0.57	0.63	0.63	0.74	0.74	0.75	0.61	0.48	0.23
Corrected Total	99.63	100.24	98.96	99.43	98.71	98.99	99.65	99.34	98.88	99.28	99.41	98.01	97.14
						Formula to 12 (Al, Si)							
F	0.00	0.00	0.00	0.00	0.00	0.00	0.00	0.00	0.00	0.00	0.00	0.00	0.00
Na	2.71	3.32	2.62	2.92	2.55	2.65	2.64	2.94	2.72	2.85	2.61	2.40	1.82
Mg	0.00	0.00	0.02	0.02	0.00	0.03	0.06	0.00	0.00	0.00	0.00	0.00	0.01
Al	3.98	3.56	4.02	3.95	4.04	4.00	3.97	3.74	3.76	3.75	3.89	4.04	4.38
Si	8.02	8.44	7.98	8.05	7.96	8.00	8.03	8.26	8.24	8.25	8.11	7.96	7.62
S	0.04	0.02	0.00	0.00	0.00	0.00	0.01	0.00	0.00	0.00	0.04	0.08	0.12
Cl	0.74	0.86	0.64	0.57	0.63	0.69	0.69	0.81	0.82	0.82	0.67	0.53	0.25
Ca	1.30	0.70	1.43	1.41	1.48	1.39	1.33	1.08	1.13	1.09	1.33	1.67	2.20
K	0.09	0.08	0.05	0.04	0.05	0.07	0.11	0.12	0.25	0.17	0.15	0.12	0.11
Fe	0.01	0.00	0.02	0.03	0.02	0.04	0.06	0.01	0.01	0.01	0.02	0.01	0.00
CO_3	0.22	0.12	0.36	0.43	0.37	0.30	0.31	0.19	0.18	0.18	0.29	0.38	0.63
Na+K+Ca	4.10	4.11	4.10	4.38	4.08	4.11	4.08	4.14	4.10	4.11	4.09	4.19	4.13

FeO : total iron; n.d.: not detected.*

Table 4

Sample ID	*Sample Name*	*Location*	*Mineralization*	*Cl (wt. %) XRFM*	*Cl (wt. %) EPMA*	*Br (ppm) XRFM*	*Na (wt. %)*	*Cl/Br molar*	*Na/Br molar*	*δ^{37}Cl (‰)*
RM01	03NUN29 125-250mm	Nunasvaara	RM	3.50	3.50	n.m.	11.99	n.m.		-0.1
RM12	Nun3.4d	Nunasvaara	RM	n.m.	3.07	n.m.	0.96	n.m.		n.m.
RM07	04 TORN 1 v. 250-500mm	Torneälven river	RM	2.60	2.71	76	9.27	770	4,238	0.3
RM08	04 TORN 1 v. 100-250mm	Torneälven river	RM	2.60	2.71	86	n.m.	680		0.0
RM05	04 TORN 2 125-250mm	Torneälven river	RM	2.50	2.74	88	8.97	639	3,622	0.3
MB02	PAH 88217 125-250mm	Pahtohavare	IOCG-M	2.78	2.92	36	9.37	1,738	9,134	0.2
MB03	PAH 88217 100-125mm	Pahtohavare	IOCG-M	2.50	n.m.	143	n.m.	393		n.m.
MB10	03PAH3 125-250mm	Pahtohavare	IOCG-M	2.80	3.07	112	9.42	565	2,935	0.2
PN20	KAL 90106 125-250mm	Kallosalmi	IOCG-PS	3.30	n.m.	55	n.m.	1,350		0.5
PN21	KAL 90106 118.4m 100-125mm	Kallosalmi	IOCG-PS	3.30	3.09	55	9.59	1,350	6,059	0.4
PN09	KAL 90107 56.38m 125-250mm	Kallosalmi	IOCG-PS	3.30	3.61	90	10.13	825	3,909	0.6
PN17	PAH 88093 100-125mm	Pahtohavare	IOCG-PS	3.30	3.41	134	10.45	554	2,709	1.0
PN18	PAH 88093 125-250mm	Pahtohavare	IOCG-PS	3.30	n.m.	90	n.m.	825		-0.1
PN16	G1-1 100-125mm	Gruvberget	IOCG-PS	2.10	2.17	38	n.m.	1,244		0.1
PN14	G1-1 250-500mm	Gruvberget	IOCG-PS	2.10	n.m.	20	n.m.	2,363		0.3
PN15	G1-1 125-250mm	Gruvberget	IOCG-PS	2.10	n.m.	38	8.29	1,244	7,580	-0.1
PN06	G4-1 125-250 mm	Gruvberget	IOCG-PS	2.70	2.92	65	9.23	942	4,971	0.1
PN19	SAR 1 125-250mm	Sarkivaara	IOCG-PS	1.00	1.32	83	6.23	271	2,609	0.9
MSW	Modern Seawater							650	600	0.0

RM: Regional Alteration Na-Cl Metasomatism, IOCG-M: IOCG-Sc altered Metabasic Rocks, IOCG-

PS: IOCG-Proximal sc-rich alt/Na Skarn.
n.m.: not measured